water

Article

Investigating the Effects of Climate and Land Use Changes on Rawal Dam Reservoir Operations and Hydrological Behavior

Sharjeel Hassan [1,2], Muhammad Umer Masood [1], Saif Haider [1,3], Muhammad Naveed Anjum [2,*], Fiaz Hussain [2], Yongjian Ding [4,*], Donghui Shangguan [4], Muhammad Rashid [1] and Muhammad Umer Nadeem [5]

1 Centre of Excellence in Water Resources Engineering, University of Engineering and Technology, Lahore 54890, Pakistan
2 Department of Land and Water Conservation Engineering, Faculty of Agricultural Engineering and Technology, PMAS-Arid Agriculture University, Rawalpindi 46000, Pakistan; engr.fiaz@uaar.edu.pk
3 Mott MacDonald Lahore, Lahore 54000, Pakistan
4 State Key Laboratory of Cryospheric Science, Northwest Institute of Eco-Environment and Resources, Chinese Academy of Sciences, Lanzhou 730000, China
5 Department of System and Information Engineering, University of Tsukuba, Tsukuba 300-1240, Japan
* Correspondence: naveedwre@uaar.edu.pk (M.N.A.); dyj@lzb.ac.cn (Y.D.)

Abstract: In order to assess the effects of climate change and land use change on Rawal Dam, a major supply of water for Rawalpindi and Islamabad, this study uses hydrological modeling at the watershed scale. The HEC-HMS model was used to simulate the hydrological response in the Rawal Dam catchment to historical precipitation. The calibrated model was then used to determine how changes in land use and climate had an impact on reservoir inflows. The model divided the Rawal Dam watershed into six sub-basins, each with unique features, and covered the entire reservoir's catchment area using data from three climatic stations (Murree, Islamabad Zero Point and Rawal Dam). For the time spans of 2003–2005 and 2006–2007, the model was calibrated and verified, respectively. An excellent fit between the observed and predicted flows was provided by the model. The GCM (MPI-ESM1-2-HR) produced estimates of temperature and precipitation under two Shared Socioeconomic Pathways (SSP2 and SSP5) after statistical downscaling with the CMhyd model. To evaluate potential effects of climate change and land use change on Rawal Dam, these projections, along with future circumstances for land use and land cover, were fed to the calibrated model. The analysis was carried out on a seasonal basis over the baseline period (1990–2015) and over future time horizon (2016–2100), which covers the present century. The findings point to a rise in precipitation for both SSPs, which is anticipated to result in an increase in inflows throughout the year. SSP2 projected a 15% increase in precipitation across the Rawal Dam catchment region until the end of the twenty-first century, while SSP5 forecasted a 17% increase. It was determined that higher flows are to be anticipated in the future. The calibrated model can also be utilized successfully for future hydrological impact assessments on the reservoir, it was discovered.

Keywords: land use classification; Rawal dam; climate change; land use/land cover change; statistical downscaling; GCMs

check for updates

Citation: Hassan, S.; Masood, M.U.; Haider, S.; Anjum, M.N.; Hussain, F.; Ding, Y.; Shangguan, D.; Rashid, M.; Nadeem, M.U. Investigating the Effects of Climate and Land Use Changes on Rawal Dam Reservoir Operations and Hydrological Behavior. *Water* **2023**, *15*, 2246. https://doi.org/10.3390/w15122246

Academic Editor: Athanasios Loukas

Received: 8 May 2023
Revised: 8 June 2023
Accepted: 10 June 2023
Published: 15 June 2023

1. Introduction

Due to the scarcity of water resources, it is necessary to guarantee everyone's survival and socioeconomic growth. The increasing population and development efforts are placing stress on the world's water resources [1]. Over the past century, water extraction has increased six fold globally, twice as quickly as population development. One-fifth of the world's population struggles with a physical water shortage, which may soon impact 500 million people [2]. According to estimates, 65% of the world's rivers and aquatic environments face imminent peril [3]. There has been devastation to the ecology and reservoirs, especially as a result of human interference [4]. Modifications to the climate have had a negative impact on flow of rivers in Pakistan [5]. Pakistan is the world's 36th most water-stressed nation. Pakistan's water supply is presently stable at 191 million acre-feet (MAF), but demand is anticipated to reach 274 MAF by 2025 [6]. Surface runoff may provide most of the water required for domestic and agricultural use.

On the other side, surface runoff has undergone significant global changes [7]. Anthropogenic activity and climate change are considered to be the two main factors affecting variations in surface runoff [6–10]. The severe fate of Pakistan's farming sector and home in addition to its manufacturing sector are indicated by the water table's declining position [11]. Drought is a global danger that can have a variety of effects, including deteriorating land conditions, wildfires, reduced agricultural output, and decreased water and air purity [12]. The duration, extent, and distribution of droughts have all risen in recent years due to global warming, increasing their detrimental effects [13]. The use of water for agriculture and industry, urbanization, deforestation, and changes in land use are examples of anthropogenic activities, occasionally referred to as human-caused environmental disturbances [14–18]. It is difficult to comprehend how climate change and human activity interact to alter streamflow, especially at the regional level [12,13]. Therefore, understanding these changes' local and regional impacts is essential for better managing water resources. The researchers developed several methods for understanding how runoff reacts to changes in the climate and in land use. These methods consist of hydrological modeling, statistical methods, and matched catchment methods. Every one of these strategies has pros and cons. For instance, scattered, semi-distributed and lumped models are often used in hydrological modeling. Since calibration and validation methods require a large number of input records, such models cannot be used in environments with barely any data. It is difficult to directly assess the effects of land use changes, and the statistical technique only provides a range of physical interpretations. Comparatively, when using paired catchment approaches, it is challenging to find two catchments with similar qualities [19]. Furthermore, there aren't many models of monthly water balance that can be easily calibrated and validated. Additionally, these models have a logical basis and require less data [20]. The ABCD hydrological model is acknowledged as a successful model over monthly temporal streamflow identification. Due to its more straightforward construction, the ABCD hydrological model performs well than other hydrological models [21]. Fewer input values are required for the ABCD model [22]. It has been widely used in studies to investigate regional water balance because of its straightforward design. This model is easier to use and has a straightforward structure [23]. However, reservoir operators are guided by reservoir operating standards when determining quantity and time for release of water. Simply put, in order to achieve the desired storage level for the season, the operator must release water as needed. The majority of the time, these regulations, which could be made up of a curve or group of curves, rely on a thorough analysis of the most important hydrologic conditions and requirements in a sequential order. A major change in the amount or pattern of inflow may have a significant impact on how well operational rules work. Through adaptation, one can at least somewhat lessen the impacts of climate change. It accomplishes this by constantly taking action to reduce climate change susceptibility. Additionally, there are limitations on its effectiveness for climate change that is occurring at a faster rate and scale.

Finding viable adaptation strategies and tackling the severity of climate change are essential to reducing the probability of disasters. Although there are adaptation options available in every sector, their potential to reduce risks associated with climate change differs between sectors and geographical areas. Although it is an excellent way to lessen effects of climate change, in the case of Xinanjiang-Fuchun-jiang reservoir, it was not possible to fully restore the system, according to Vonk et al.'s [24] analysis of a Xinanjiang-Fuchun-jiang reservoir's operational plans under several climate change scenarios.

Researchers and water resources managers have conducted many studies to better understand and manage the potential consequences of climate and land use changes on hydrology of different watersheds [10,25–30], but these studies lack the knowledge of how this change in inflows will affect the operational strategies under which different reservoirs are operated. Although changes in streamflows can directly impact water availability, affecting various sectors such as agriculture, industry, and domestic water supply, simultaneously, reservoirs also play a critical role in water storage, flood control, and hydropower generation. Climate and land use changes can affect the inflow patterns and sedimentation rates, thereby impacting reservoir operations and their ability to meet water supply demands, prevent flooding, and generate clean energy. Assessing these impacts is essential for optimizing reservoir operations and ensuring their long-term sustainability.

The simulations of rainfall and runoff frequently use the semi-distributed hydrological conceptual model HEC-HMS [31–33]. In order to simulate runoff in short-term as well as long-term settings, HEC-HMS uses traditional techniques [34,35]. Other studies have shown that HEC-HMS models streamflow using widely available data and catchment types [36–39]. Additionally, a significant number of scholars have used the HEC-HMS to simulate rainfall and runoff in order to study how changes in land use and the climate affect the runoff pattern. For attribution reasons, results from using HEC-HMS globally are acceptable [40,41]. Therefore, in the current study, it was decided to carry out attribution analysis using HEC-HMS. Researchers and water resource managers have used a variety of methods and models for attribution analysis. However, there are always some ambiguities and differences because every strategy and paradigm yields unique results [42,43].

In the present research, consequences of anthropogenic activities and climatic effect are considered separately. The watershed is particularly vulnerable to the effects of climate change and human intervention in the humid region [44]. As a consequence, the current study is concentrated on the Rawal watershed, a humid watershed in the Margalla Hills. The water supply from these basins is primarily used to feed Rawalpindi, a neighboring city, and Islamabad's capital with drinking water. Over the past few decades, there have been major changes in the land use in these basins. The following are the study's primary goals: (a) Evaluation of future water supply in light of the climate change forecasts. (b) Investigation of how urbanization affects Rawal Dam discharge rates. (c) Optimization of various operational strategies for the Rawal reservoir in view of climate change.

2. Study Area

Pakistan's Potohar Plateau is home to Rawal Dam (Figure 1). The reservoir's main river, the Kaurang River, gets water from 43 smaller streams and four minor tributaries. While some of these waterways have springs in their beds known as Kathas, others have perennial flows. Along the section of the Kaurang River, dry nullahs known as Kassis are also commonly encountered in addition to Kathas. The study location is located in Pakistan's subtropical region. Rawal Dam is located in Pakistan's Southern Himalayas, with coordinates of 73°3′–73°24′ E and 33°41′–33°54′ N and a 273 km^2 watershed. The watershed's elevation varies from 523–2145 m, and 47% of the Rawal Dam's catchment area is in Islamabad, 43% is in Punjab, and 10% is in Khyber Pakhtunkhwa.

The study region has a predominantly humid subtropical climate with mean annual rainfall of about 1220 mm. The Margalla Hills, a significant portion of the catchment region, occasionally experience snowfall from November through February. With temperatures varying from 36 to 42 °C in June and July, and from 3 to 5.5 °C in December and January, respectively, those months are the warmest and coldest of the year. The area experiences extreme temperatures between −4 °C and 48 °C. There are two rainy seasons in the area. Winter rains fall in the months of January through March, while summer rains, or monsoon season, which account for about 60% of total rainfall, fall in the months of July through September. Simli, Khanpur Dam, and Rawal Lake all control Islamabad's temperature.

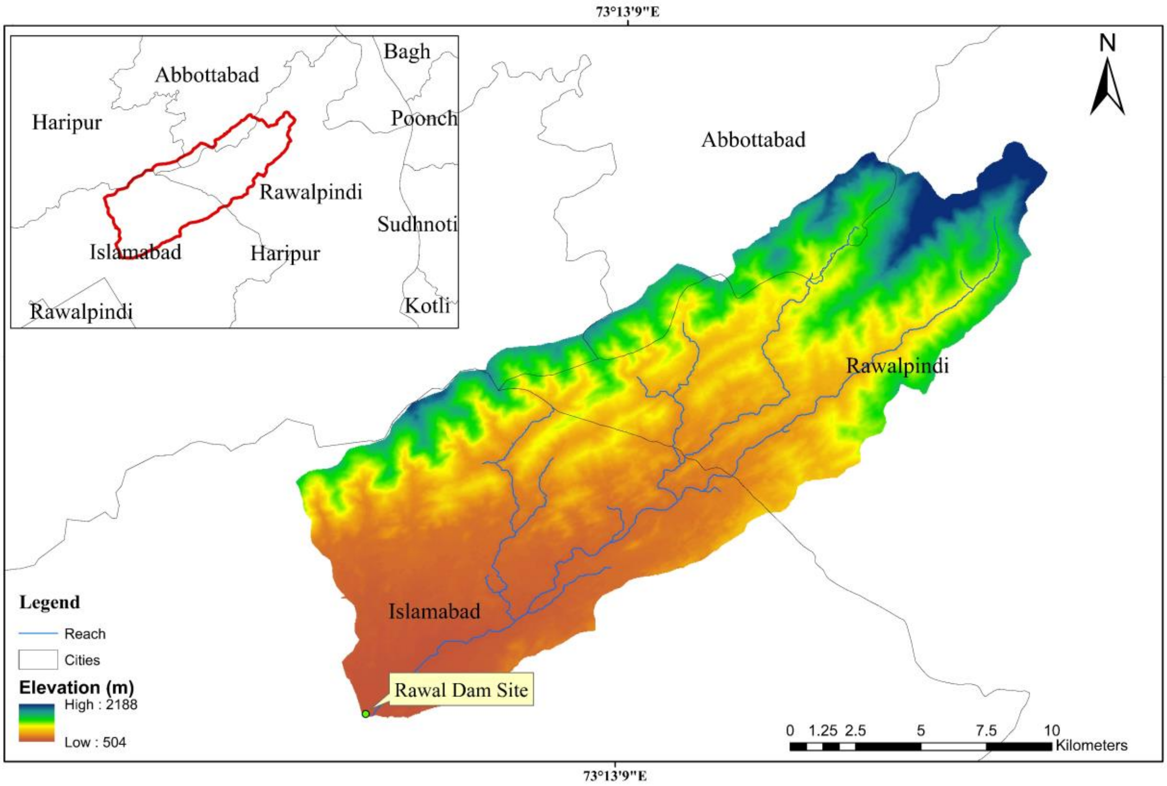

Figure 1. Location and elevation data of Rawal Dam catchment area.

One of the major water supply sources for the twin towns of Rawalpindi and Islamabad, the Rawal Dam provides about 23 MGD of water. Water from Rawal Dam is used to irrigate a 500-acre command area in addition to being used for consumption. This water supply has been negatively impacted by rising population, evaporation, and other losses. In 1992, Rawal Lake had an area of 594 hectares, but it is now only 478 hectares. This indicates that in the past three decades, the lake's size has decreased by 19.5%.

3. Materials and Methods

3.1. Datasets

3.1.1. Hydro-Meteorological Data

The data on rainfall was gathered from three climatic sites. For the years 1990 to 2015, the Pakistan Meteorological Department (PMD) supplied daily data for the stations at Murree and Islamabad (zero point), and the Small Dams Organization did the same for Rawal Dam. All three stations have used historical data from 1990 to 2015 as a baseline time.

3.1.2. Remote Sensing Data

For the purpose of delineating the Rawal Dam catchment and extracting physical characteristics like elevation, slope, catchment area, etc., USGS Earth Explorer provided a Digital Elevation Model (DEM) of Rawal Dam and its watershed with a resolution of 30 m along with Landsat imageries.

This study utilized data from Landsat 8 (OLI) and Landsat (4–5) (TM), employing bands 8 and 7, respectively, to distinguish between changes in land use and land cover within the Rawal Dam catchment area for three independent time periods, i.e., 2000, 2010, and 2020. Seasonal distribution and vegetation deviation were taken into consideration when choosing the picture times. All pictures were obtained from the USGS Earth Explorer website and saved as .tiff files.

3.1.3. Climate Projected Data

Based on spatial resolution, a global circulation model called MPI-ESM1-2-HR was chosen for this research. SSP2 and SSP5, two Shared Socioeconomic Pathways (SSPs), were taken into consideration. The sixth evaluation report of the Inter-Governmental Panel on Climate Change (IPCC) contains information about this GCM. The large-scale grid-like GCM data were downscaled in order to project the climatic conditions at a local scale. By establishing quantitative relationships between the local climatic variable and the large-scale GCM climatic variables, statistical downscaling was carried out. The interpretation of statistical downscaling is much simpler than that of dynamic downscaling. However, past climatic data and gauged data are extremely important for statistical downscaling. For the downscaling of temperature and precipitation in this study, a distribution mapping (multiplicative for precipitation and additive for temperature) approach was used.

A popular bias correction method used in many climate change studies is distribution mapping (DM). Replicating a transfer function from the gauged data to the mean monthly value of the GCMs data is the basic idea behind how it operates. To rectify the skew from the downscaled future GCMs data, the gamma transfer function and the gaussian transfer function for precipitation and temperature data, respectively, need to be downscaled.

3.2. Methodology

This research work employs a systematic methodology to investigate the impacts of climate and land cover changes on reservoir operational strategies and hydrology of Rawal Dam of Pakistan. The methodology includes data collection, downloading GCM-simulated meteorological data and downscaling it for Rawal Dam catchment, hydrological modeling, and integration of various factors to provide a comprehensive understanding of the complex interactions and implications for water resource management. Figure 2 depicts the flowchart of methodology adopted for this study.

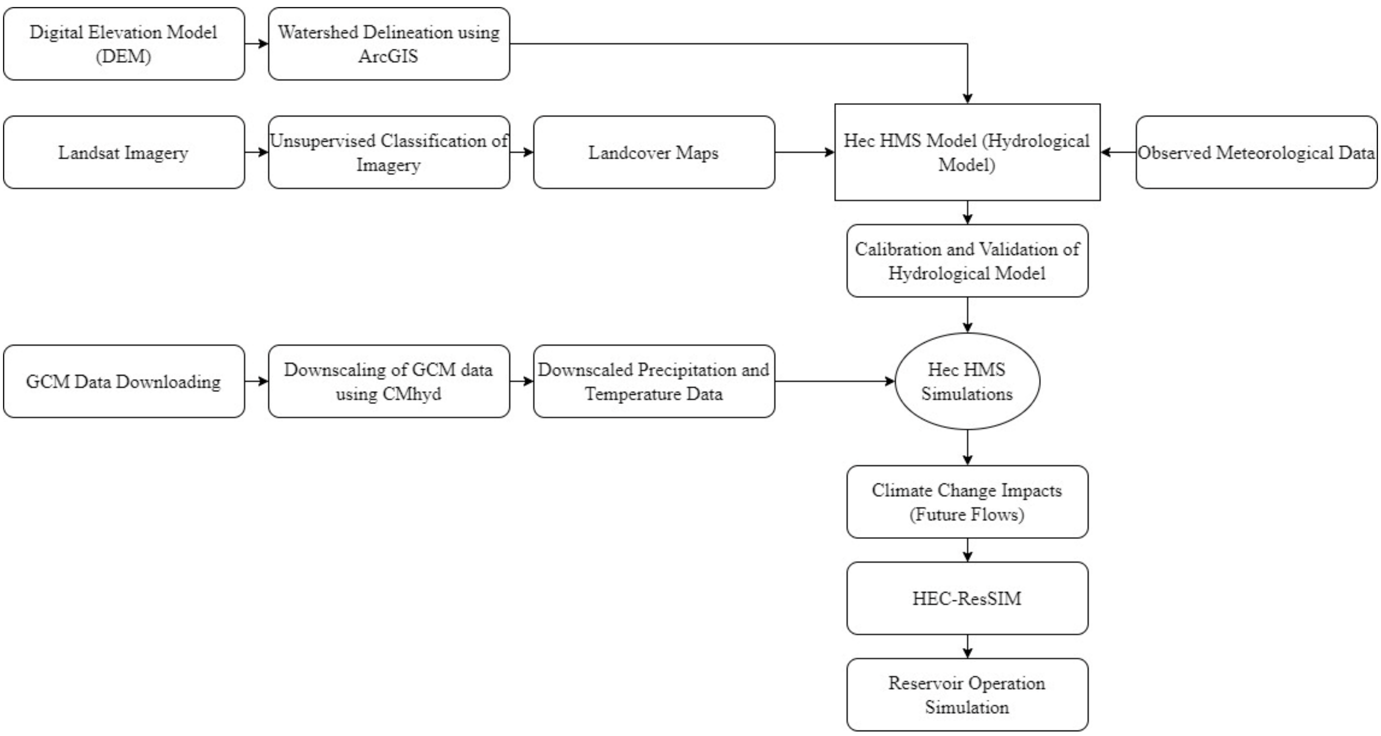

Figure 2. Methodology flowchart.

3.2.1. Statistical Downscaling

GCM-based forecasts of temperature and precipitation at the size of the river basin were subjected to bias correction using the CMhyd model [45,46]. It has been used to reduce bias between gauge-based actual climatic variables and GCM-based projected climatic variables in various regions of the world [47]. According to the study of Anandhi et al. [47], any river-basin-size hydro-climatological investigation can successfully and continuously reduce the output of the GCM utilizing the CMhyd model. Numerous statistical downscaling methods for temperature and precipitation are offered by the CMhyd. In this study, the distribution mapping strategy was employed for precipitation, while the power transformation technique was utilized to downscale the results of the Global Climate Models for temperature under SSP2 and SSP5 circumstances. In this context, time series data over the daily anticipated precipitation, minimum, maximum temperatures were obtained by combining the daily rainfall, maximum, minimum temperatures over baseline period (1990–2015) and the study's future time period (2016–2100). These data also included anticipated calculations of GCMs.

Distribution mapping is a statistical downscaling technique used to estimate local-scale climate variables based on the relationship between large-scale climate information and observed local variables. It involves mapping the probability distribution function of the large-scale climate variable onto the observed local variable distribution, allowing for the generation of downscaled climate projections at finer spatial scales. However, power transformation is a statistical downscaling technique that involves transforming the data using a power function to account for nonlinear relationships between large-scale and local-scale climate variables. By applying power transformation, it helps to capture the nonlinearities and improve the relationship between the variables, enabling more accurate downscaling of climate projections.

3.2.2. Image Classification

Maps of current and historical land use and cover were created using an unsupervised image classification algorithm. Downloaded Landsat imagery from various years was examined in ArcGIS, and then five classes—vegetation, built-up areas, water, forests, and barren land—were identified using the isocluster unsupervised image classification technique, which is an unsupervised image classification algorithm that is commonly used for segmenting and categorizing image data based on spectral properties. It operates by iteratively grouping pixels with similar spectral characteristics into clusters. IsoCluster takes advantage of the statistical properties of the image data, such as pixel intensities or spectral signatures, to identify distinct regions or objects within an image. The algorithm starts by randomly selecting initial cluster centers and assigns pixels to the nearest cluster based on their spectral similarity. It then updates the cluster centers based on the mean of the pixels assigned to each cluster. This process continues iteratively until convergence is achieved, ensuring that pixels are accurately classified into clusters. IsoCluster is particularly effective in scenarios where there is a clear distinction in spectral properties among different regions or objects in the image, making it a valuable tool for applications such as land cover classification, object detection, and image segmentation.

3.2.3. Hydrological Modeling

ArcGIS, a spatial analytic program, was used to pre-process the delimited watershed and extract terrain data. The watershed was given the correct coordinate system, or WGS 43N. Basin characteristics, such as river slope, the length of the river, the size of the basin, and the stream lines, were derived. According to physical characteristics, the accumulation of flow, flow direction, and the convenience of measuring sites, the catchment of Rawal Dam was separated into six sub-basins.

The separated basin was then imported into HEC-HMS for hydrological modeling. It is a widely used software tool developed by the U.S. Army Corps of Engineers. Designed for hydrologic modeling and analysis of watershed systems, HEC-HMS enables engineers and hydrologists to simulate and predict the behavior of complex hydrological processes such as rainfall, runoff, evapotranspiration, and streamflow. With its user-friendly interface and comprehensive set of features, HEC-HMS allows for the creation of detailed hydrologic models by defining watershed characteristics, rainfall patterns, land use, and soil properties. The software incorporates various methods for runoff and streamflow routing, including the SCS Curve Number method, unit hydrographs, and Muskingum–Cunge routing. HEC-HMS facilitates the analysis of different hydrological scenarios, aiding in flood forecasting, water resource planning, and floodplain management.

In addition to the Rawal Dam's daily inflows, daily temperature, and precipitation data for the Islamabad (zero point) station, Murree Station, and Rawal Dam were introduced. The parameters of the model were carefully adjusted until a successful simulation versus the observed data was obtained. The model was initially calibrated for the years 2003 to 2005. The outcome validation step was carried out using the same parameters. The same settings were used for the results validation stage. Validation took place between 2006 and 2008.

3.2.4. Model Performance Evaluation

The effectiveness of the HEC-HMS model was assessed using assessment markers for percent bias (*PBIAS*), coefficient of determination (R^2), root mean square error (*RMSE*) and Nash–Sutcliffe efficiency (*NSE*) [48]. Higher values of R^2, which runs from −1 to 1, suggest greater simulation performance. The range of *NSE* values is 0 to 1, with values over 0.50 regarded as acceptable. Greater values represent lower simulation error [49]. Readings on the *PBAIS* between −15% and +15 are seen as appropriate. The R^2, *NSE* and *RMSE* mathematical expressions are shown below.

$$R^2 = \frac{\left[\sum\left(Q_m - \overline{Q_m}\right)\left(Q_s - \overline{Q_s}\right)\right]^2}{\sum\left(Q_m - \overline{Q_m}\right)^2 \sum\left(Q_s - \overline{Q_s}\right)^2} \quad (1)$$

$$NSE = 1 - \frac{\sum\left(Q_m - \overline{Q_s}\right)^2}{\sum\left(Q_m - \overline{Q_m}\right)^2} \quad (2)$$

$$RMSE = \sqrt{\frac{\sum_{i=1}^{n}\left(Q_m - Q_s\right)^2}{n}} \quad (3)$$

where Q_s, Q_m, $\overline{Q_m}$, and $\overline{Q_s}$ stand for simulated discharge, measured discharge, average measured discharge and average simulated discharge.

3.2.5. Model for Reservoir Simulation Application (HEC-ResSIM)

The Hydrologic Engineering Center of the USACE created the reservoir system modeling HEC-ResSIM to optimize reservoir operations for different operational goals and constraints [50]. Because it attempts to mimic the decision-making procedures that reservoir management has historically used to schedule water releases, HEC-ResSIM stands out among reservoir simulation models [51]. It offers users access to three main sets of capabilities, known as modules that enable access to various types of data inside a watershed. These elements consist of reservoir network, simulation, and watershed configuration. The user's manual contains a full explanation of the model's construction [50].

The HEC-ResSIM model's main inputs include the Rawal reservoir's physical properties, reservoir operating rule curves, and daily measured inflow. The filtration plant and spillway's discharge capacity as well as the reservoir's elevation–area relationship (based on hydrographic surveys from 2004 and 2013) are used to describe the reservoir system's physical features. The operational rule curves were built using several operational and storage zones of the Rawal reservoir that CDA detected using the HEC-ResSIM model (Figure 3). The operating zones (Zone 1, Zone 2, and Zone 3) are divided into their corresponding subsets by two rule curves that display reservoir goal levels that must be reached in corresponding months. CDA created these operational zones under the presumption that a safe yield would be a full supply of 2.05 cumecs (39 MGD) from the Rawal reservoir. Figure 3 shows three conditional releases based on reservoir levels: (1) if the reservoir level is in Zone 1, the reservoir should release 2.05 cumecs of water at full capacity. (39 MGD); (2) if the reservoir level is in Zone 2, the supply should be reduced by 25% to 1.54 cumecs (29.25 MGD); and (3) reduced supply should be kept at 1.025 cumecs (19.5 MGD) if reservoir level is in Zone 3. A spillway with a 1275 cumec discharge capacity is used to release any extra water when Rawal reservoir reaches its maximum water level (MWL) during the summer monsoon. HEC-ResSIM simulated daily reservoir levels for the years 2004 to 2013 once the original data had been entered, and it then compared those levels to the actual reservoir levels.

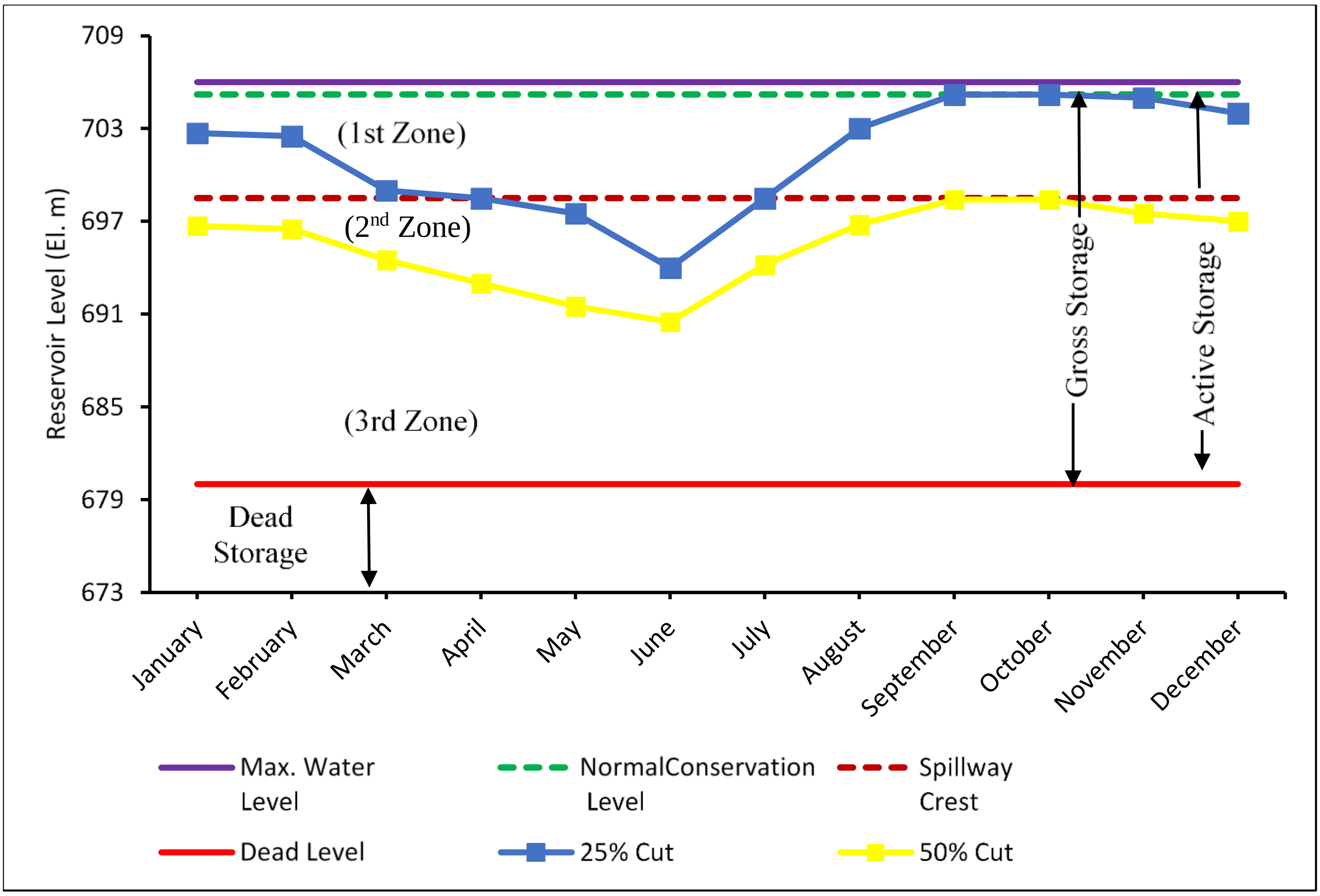

Figure 3. Operational rule curves for Rawal Dam reservoir.

4. Results

4.1. Downscaling of Future Climate Data

The main elements of climate systems and how they interact can be represented mathematically in detail by global climate models (GCMs). They divide the atmosphere of world into 100- to 200-km-wide grid boxes. For each grid, equations describing atmospheric dynamics are solved. Due to the fact that surface topography is also resolved at the same spatial scales (100–200 km), several significant physical processes and meteorological phenomena cannot be accurately represented. Thus, bias adjustment of the GCM data downloaded is necessary.

To determine how the future climate would affect the amount of water available at Rawal Dam, the climatic data obtained from a GCM model was statistically downscaled to the stations at Islamabad (zero point), Rawal Dam and Murree. It was decided to use 1990 to 2015 as the baseline. The subsequent evaluation of future climate effects used the updated precipitation data.

4.2. Potential Shifts in Rainfall and Temperature

The anticipated data were scaled down until end of the twenty-first century after the GCM and downscaling methods for the rainfall and temperature (max and min) were chosen. For anticipated precipitation and temperature, two datasets were created: a baseline dataset for the years 1990 to 2015 and a future dataset for the years 2016 to 2100. (e.g., SSP2 and SSP5).

4.2.1. Projection of Mean Maximum Temperature

The maximum temperature in the Rawal Dam catchment area is expected to rise from 25.8 °C during the baseline era (1990–2015) to 26.9 °C under SSP2 and 28.5 °C under SSP5, representing increases of 4.3% and 10.6%, respectively, by the end of the twenty-first century (Table 1). A periodic examination of this shift was performed using the division of the year's months into four seasons—winter being represented by the months of November, December, and January, and spring by the months of February, March, and April. May, June, and July are considered summer months, while August, September, and October are considered autumnal months).

Table 1. Summary of change in hydrology in Rawal Dam's catchment area caused by climate change.

Climate Scenarios	Precipitation		Maximum Temperature		Minimum Temperature		Flows (Current Land Use Land Cover Future Climate)			Flows (Future Land Use Present Climate)	
	mm	% Change	°C	% Change	°C	% Change	Cusecs	% Change		Cusecs	% Change
Observed	1414.5	-	25.8	-	13.5	-	129.5	-	Observed	129.5	-
SSP2	1817.1	12.5	26.9	4.3	14.6	8.2	151.9	13.77			
SSP5	1852.2	19.2	28.5	10.6	16.1	19.8	160.5	16.29	Future	177.1	36.8

According to the examination of seasonal fluctuation in Figure 4, the highest temperature was higher for each of the four seasons. According to Figure 4, under SSP2 and SSP5, the wintertime maximum temperature rose from 14.06 °C to 14.86 °C and 15.63 °C. Under SSP2 and SSP5, the maximum autumn temperatures increased from 21.91 °C to 22.83 °C and 23.6 °C, respectively, whereas SSP2 increased the maximum summer temperatures from 24.7 °C to 25.59 °C and 26.36 °C. Under SSP2 and SSP5, respectively, springtime maximum temperatures increased from 16.71 °C to 17.4 °C and 18.17 °C.

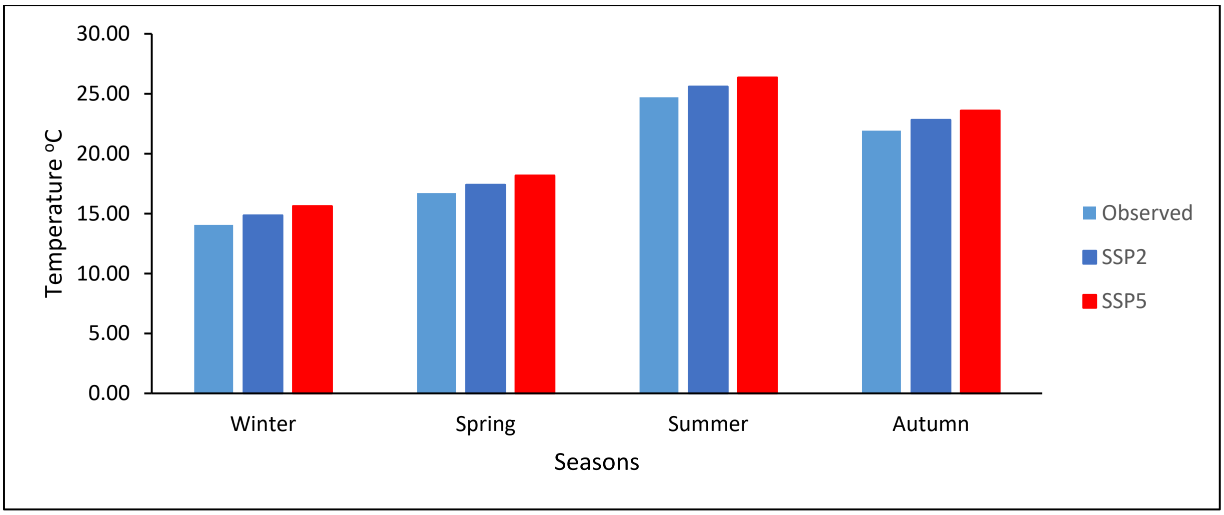

Figure 4. Seasonal change in maximum temperature of Rawal Dam's catchment area under two Shared Socioeconomic Pathways (SSP2 and SSP5).

4.2.2. Projection of Mean Minimum Temperature

The lowest temperature in Rawal Dam catchment area is predicted to rise from 13.5 °C under the baseline time frame (1990–2015) to 14.6 °C under SSP2 and 16.1 °C under SSP5, respectively, up until the end of the twenty-first century. Divided into four seasons, the months of the year were used to analyze this development from a seasonal perspective (spring is February, March, and April, while winter is November, December, and January. May, June, and July are considered summer months, while August, September, and October are considered autumnal months).

According to Figure 5's research of seasonal variance, the minimum temperature increased across the year's four distinct seasons. According to Figure 5, under SSP2 and SSP5, the winter minimum temperature rose from 3.6 °C to 4.4 °C and 5.2 °C. Summer maximum temperatures increased from 15.7 °C to 16.5 °C under SSP2 and 17.2 °C under SSP5, while autumn maximum temperatures increased from 10.7 °C to 11.5 °C and 12.2 °C under SSP2 and SSP5, respectively. Under SSP2 and SSP5, the highest spring temperatures rose from 7.1 °C to 7.9 °C and 8.6 °C, respectively.

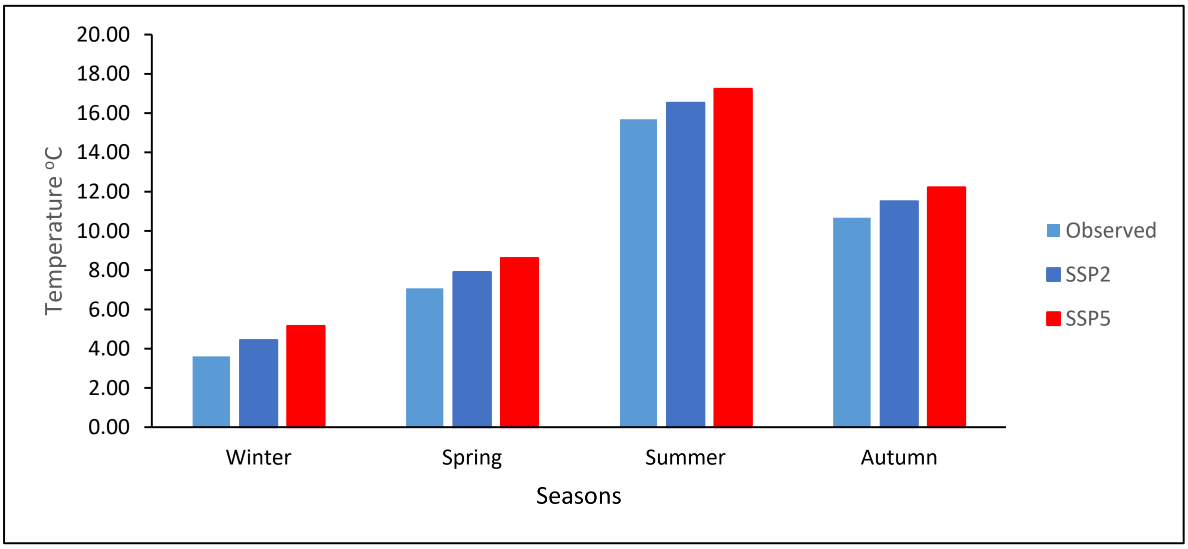

Figure 5. Seasonal change in minimum temperature of Rawal Dam's catchment area under two Shared Socioeconomic Pathways (SSP2 and SSP5).

4.2.3. Projection of Precipitation

Precipitation in the Rawal Dam catchment area is expected to increase from 1414.5 mm in the baseline time period (1990–2015) to 1591.3 mm and 1686.1 mm, respectively, by end of the twenty-first century, representing increases of 12.5% and 19.2%. Divided into four seasons, the months of the year were used to analyze this development from a seasonal perspective (spring is February, March, and April, while winter is November, December, and January. May, June, and July are considered summer months, while August, September, and October are considered autumnal months).

According to the analysis of seasonal variation illustrated in Figure 6, there was a rise in precipitation throughout the summer, winter, and fall and a decrease in precipitation throughout the spring. It was shown that under SSP2 and SSP5, winter precipitation rose from 45.3 mm to 47 mm and 54 mm. Precipitation in the summer and autumn followed a similar trend, but with a more pronounced increase. For example, in the summer, it increased from 157.3 mm to 228.5 mm under SSP2 and 222.9 mm under SSP5, while in the autumn, it increased from 170.8 mm to 236.7 mm and 252.5 mm under SSP2 and SSP5, respectively. On the other hand, under SSP2 and SSP5, the amount of precipitation projected to fall in the Rawal Dam catchment region in the spring is anticipated to drop from 106.4 mm to 93.5 mm and 88 mm, respectively.

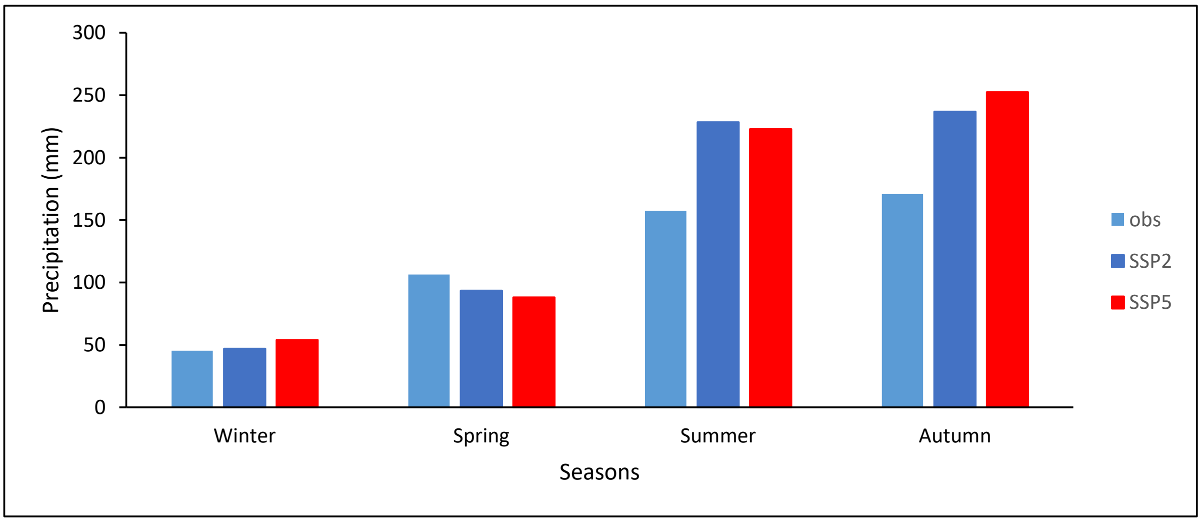

Figure 6. Seasonal change in precipitation of Rawal Dam's catchment area under two Shared Socioeconomic Pathways (SSP2 and SSP5).

4.3. Land Use Land Cover Change Trends

Using the image categorization tool in ArcGIS, the mosaicked Landsat 2000, 2010 and 2020 images were classified in an unsupervised manner. Figure 7 provides classified maps of the study region. The pictures were grouped into five categories: water, vegetation, barren land, forests, and populated areas. The findings showed that between 2000 and 2020, the areas of vegetation, forest, barrenness, and water bodies in the catchment of Rawal Dam declined by 9.2%, −8.5%, −12.3%, and −1.3%, respectively. Meanwhile, the built-up area, the fifth land use land cover class, saw a rise of 31.3%, which is a significant increase. Table 2 shows this shift in land use and cover groups.

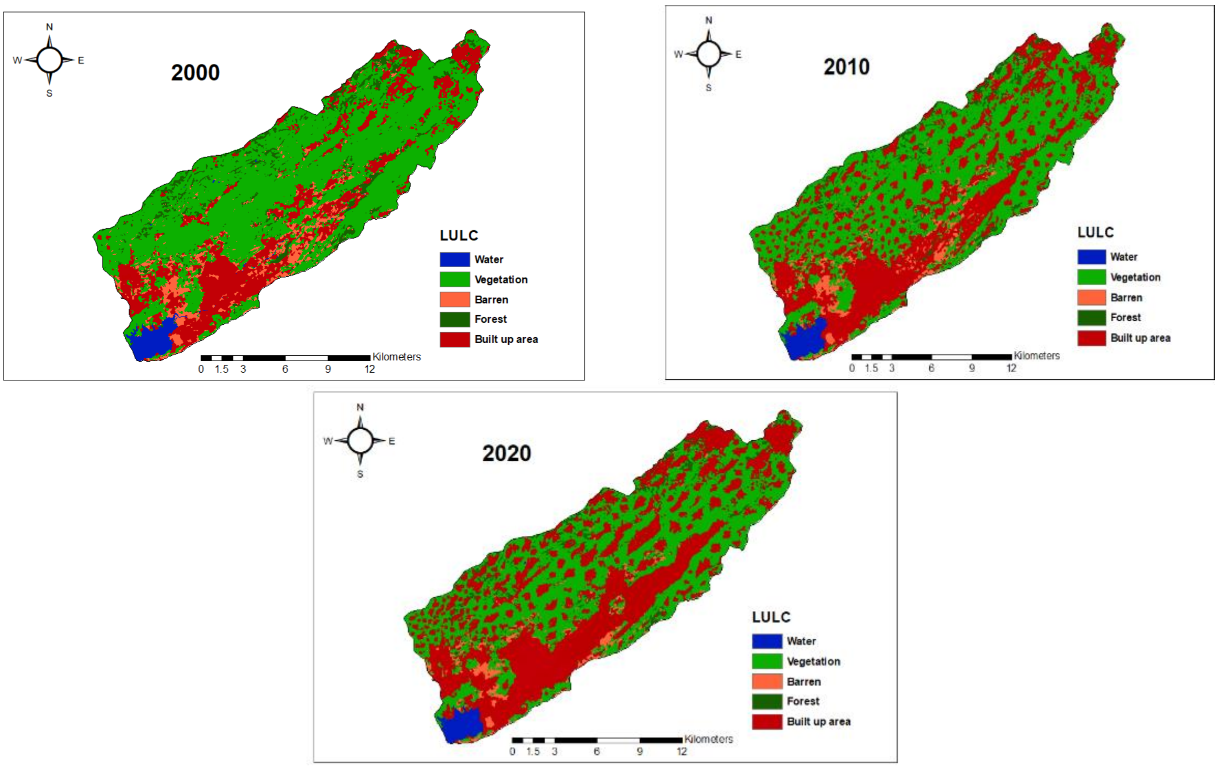

Figure 7. Land use/Land cover maps of Rawal Dam's catchment area for the years 2000, 2010, and 2020.

Table 2. Trends of different land use land cover classes in Rawal Dam's catchment area.

Land Use Land Cover Classes	2000		2010		2020		Change in Land Use (2000–2020)
	Area (km^2)	Percent Area	Area (km^2)	Percent Area	Area (km^2)	Percent Area	
Vegetation	103.5	37.9	89.3	32.7	78.4	28.7	−9.2
Forest	69.4	25.4	60.8	22.3	46.3	17.0	−8.5
Water	5.7	2.1	3.2	1.2	2.2	0.8	−1.3
Bare soil	75.1	27.5	58.8	21.5	41.4	15.2	−12.3
Built up area	19.3	7.1	60.9	22.3	104.7	38.4	31.3
Total	273	100	273	100	273	100	0

Projected Land Use Land Cover

The ArcGIS image classification tool was used to create land use and land cover maps for the years 2000, 2010, and 2020. The arithmetic extrapolation method was then used to evaluate the urbanization trend in the Rawal catchment.

It was expected that the built-up area would be 19.3 km^2 in 2000, 60.9 km^2 in 2010, and 104.7 km^2 in 2015 using maps of the study region's land use and land cover. Using the unit approach, it was predicted that the built-up area of the Rawal watershed will grow to 161.63 km^2 by 2040, representing an increase of 85.4 km^2 overall over that time frame.

4.4. Calibration and Validation of Hydrological Model

For hydrological modeling, several academics and experts have employed the HEC-HMS model. Hydrological modeling of the Rawal Dam catchment region was performed for the years 2016–2100 to evaluate the impact of the relationship between climate change and land use land cover on the water availability of catchment region. The model has been calibrated and validated through this process.

The Korang River was used for model calibration and validation at the Rawal Dam site. The process of calibration involves finding the ideal set of parameters that best match the observed and simulated discharge. The model was initially run in daily time steps, followed by calibration for the years 2003 to 2005 and validation for the years 2006 to 2008. Table 3 displays the calibration's input variables.

Table 3. Description of parameters and their adopted values used for calibration and validation.

Sub-Basin	Initial Deficit (mm)	Max Storage (mm)	Constant Rate (mm/h)	Time of Concentration (h)	Storage Coefficient (h)	Recession Constant
1	15	30	2.3	3	9	0.89
2	15	30	2.2	3	9	0.89
3	15	30	1.8	2.5	6	0.89
4	15	30	1.9	2.5	6	0.89
5	15	30	1.5	2.5	4	0.89
6	15	30	1.4	2	4	0.89

The daily and monthly discharges were accurately reproduced by the model. The model is effective at simulating the low, middle, and peak flows. Figures 8 and 9 demonstrate the calibration and validation for Korang River, respectively. The measured and predicted discharges show a respectable degree of agreement after the HEC-HMS model's calibration and validation. Table 4 provides values of Nash–Sutcliffe coefficient, RMSE and determination R^2 for calibration and validation.

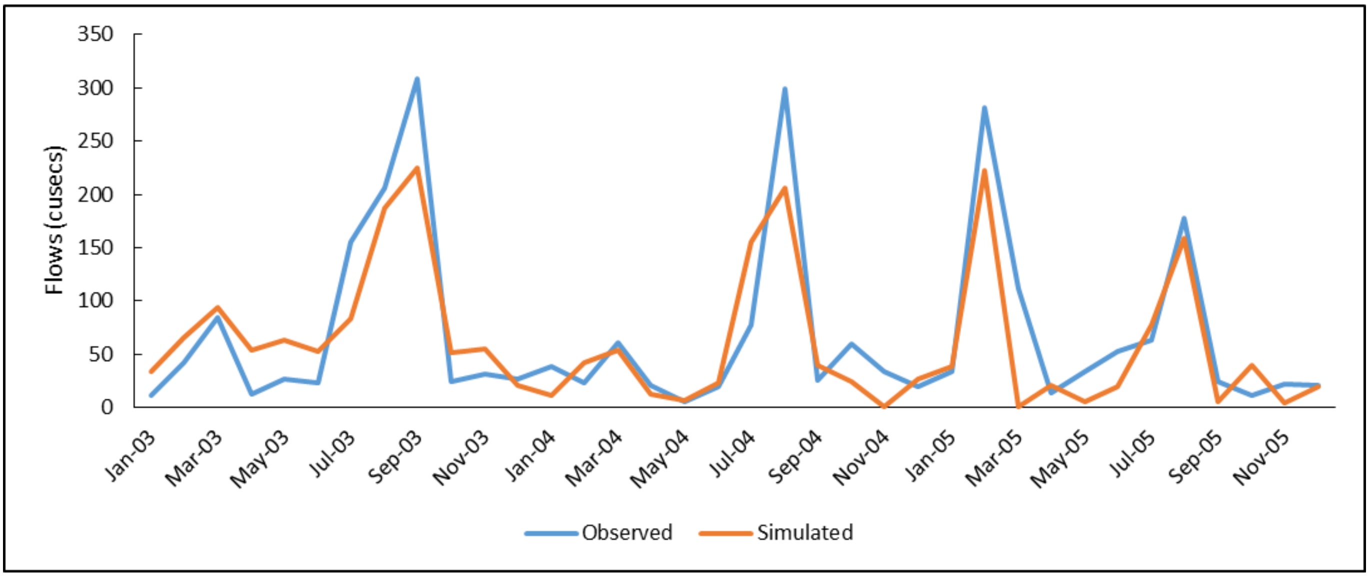

Figure 8. Comparison between observed and simulated flows (cusecs) in the calibration period (2003–2005).

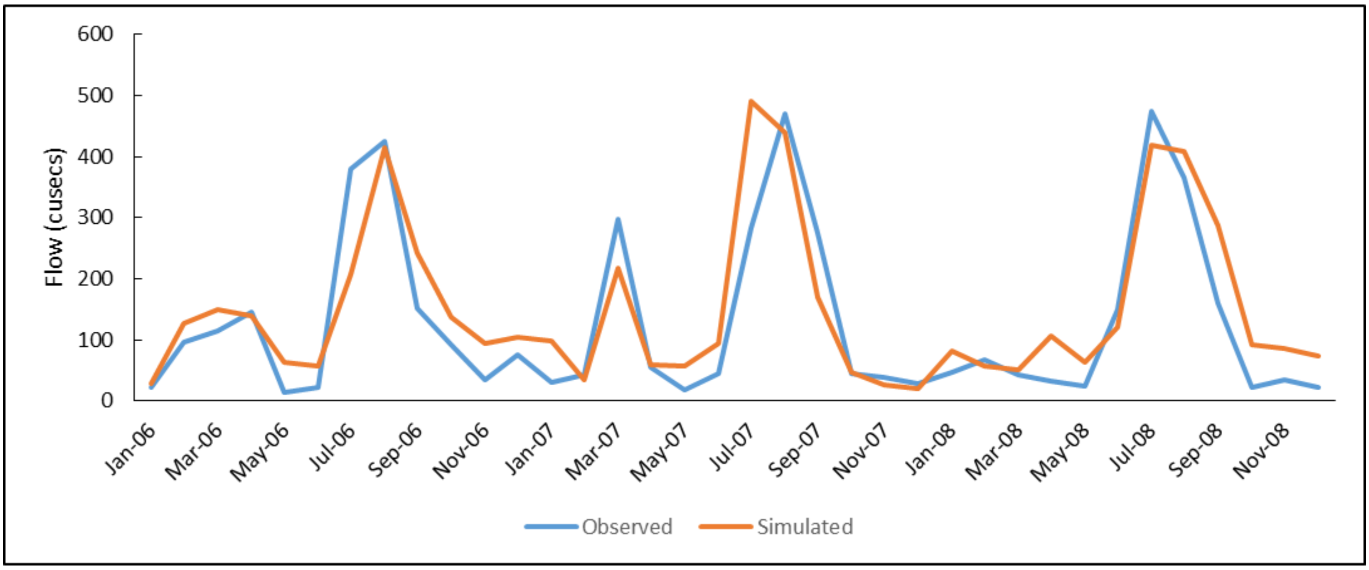

Figure 9. Comparison between observed and simulated flows (cusecs) in the validation period (2006–2008).

Table 4. Statistical summary of calibration and validation of the hydrological model.

Parameters	Calibration	Validation
NSE	0.78	0.77
R^2	0.81	0.79
RMSE	1.98	2.4

4.5. Impact of Projected Climate on Flows

This arrangement was used to anticipate future flows on an annual basis for the years 2016 to 2100 once the model had been calibrated and validated. The future flows under two scenarios were evaluated.

Hypothetical Scenarios A and B: hydrological reaction to future climate and present land use (hydrological response under current climate and projected land use).

Considering projected climate and current land use, Scenario A examines the hydrological response.

Up to the end of the twenty-first century, flows based on climate change were predicted using the calibrated model. The greatest temperature growth was reached under SSP2 and SSP5, by 4.3% and 10.6%, respectively, while the lowest temperature increased by 8.2% to 19.8%, whereas precipitation rose by 12.5% and 19.2%. In Table 5, it is estimated that under SSP2 and SSP5, the fluxes will grow from 129.5 cusecs in baseline period (1990–2015) to 151.9 cusecs and 160.5 cusecs, respectively, in the future time horizon (2016–2100). Under constant land use circumstances (current), this variation in temperature and precipitation was forced into the calibrated HEC-HMS model.

Table 5. Percentage change in inflows at Rawal dam under Scenario A (i.e., future climate and current land use).

Climate Scenarios	Flows (Current Land Use Land Cover Future Climate) (2016–2100)	
	cusecs	% change
Observed	129.5	-
SSP2	151.9	13.8
SSP5	160.5	16.3

Figure 10 relates the mean monthly flows for the baseline period (1990–2015) to the flows over the future time horizon under SSP 2 and 5 scenarios to examine temporal variations in mean monthly flows in the Rawal Dam catchment. Throughout the entire year, both SSPs anticipate an increase in the flow, with the exception of the months of February, April, September, and December. Both SSP 2 and SSP 5 showed a decline in the flow of January and February, but the flow of April and September grew under SSP 2 but fell under SSP 5, respectively.

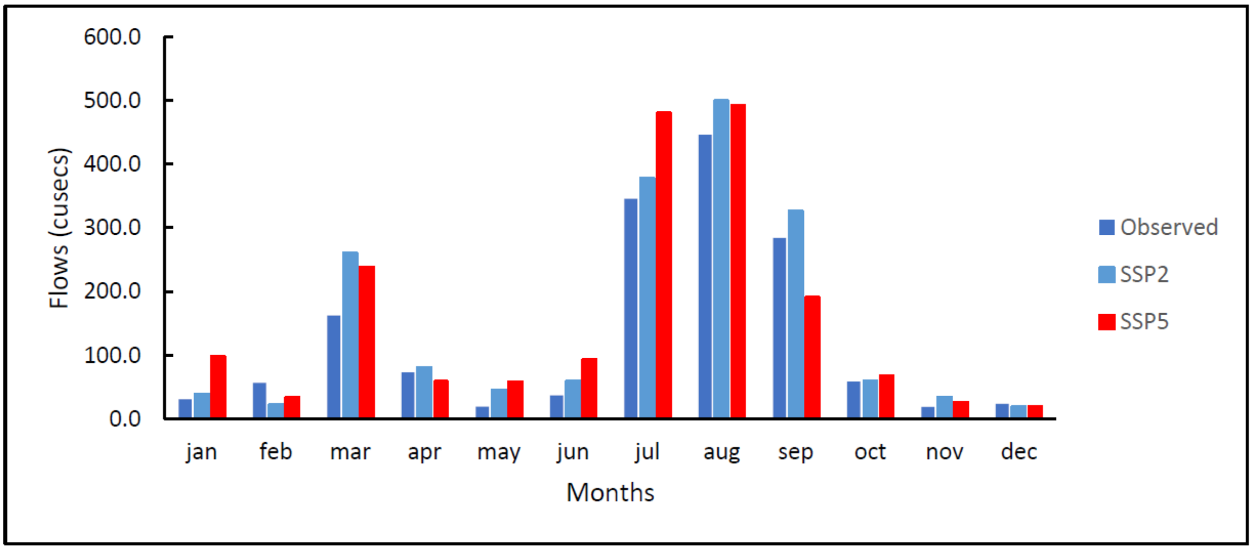

Figure 10. Mean monthly flows at Rawal Dam under future climate and current land use conditions.

The increase in precipitation, maximum temperature, minimum temperature, and built-up area collectively contributed to the increase in streamflows. Firstly, an increase in precipitation directly influences streamflows by introducing a larger volume of water into the hydrological system. Higher levels of rainfall or snowfall result in increased runoff, with the excess water flowing into streams and rivers, thus raising their water levels and streamflows. This intensified precipitation can be attributed to climate change, which alters weather patterns and leads to more frequent and intense rainfall events.

Secondly, warmer minimum temperatures affect the timing and distribution of precipitation. In regions where temperatures are close to the freezing point, a shift from snowfall to rainfall occurs, reducing water storage in the form of snowpack. The transition to rain during winter results in a more direct water input into water bodies, further increasing streamflows.

In addition to climate-related factors, the expansion of built-up areas can also influence streamflows. Urbanization and the increase in impervious surfaces, such as concrete and asphalt, reduce the natural infiltration of water into the ground. As a result, more rainfall becomes surface runoff, quickly entering streams and rivers, and leading to higher streamflows. The expansion of built-up areas often involves the alteration or construction of drainage systems, which can further modify the flow paths of water, potentially increasing streamflows in certain areas.

In summary, the increase in precipitation, maximum temperature, minimum temperature, and built-up area collectively contribute to the rise in streamflows. Climate change-induced changes in precipitation patterns, coupled with higher temperatures, influence the amount and timing of water entering water bodies. Additionally, urbanization and the expansion of built-up areas alter the natural flow of water, resulting in increased surface runoff and subsequent streamflow augmentation.

Scenario B: hydrological response in light of future land use and current climate.

The calibrated model was then used to estimate flows based on future climate and future land use change after flows were predicted for the future climate and existing land use.

According to land use patterns, between 2000 and 2020, the built-up area of the Rawal Dam basin expanded by 31.3%. Considering that 70% of the overall urban area is impervious and another 20% is in the form of house lawns, etc., this shift in urbanization was subsequently extended and incorporated into the model as imperviousness with a factor of 0.7. Meanwhile, the percentages of other land use types, such as forests, vegetation, arid terrain, and water, fell by 8.5%, 9.2%, 12.3%, and 1.3%, respectively. This change in land use and the climatic variables observed during the base line era (1990–2015) are then fed into the calibrated HEC-HMS model under increasing imperviousness to assess effects of urbanization on flows at Rawal Dam. The statistics predict that flows will rise by 36.8% from the baseline era (1990–2015) value of 129.5 cusecs to 177.1 cusecs (Table 6).

Table 6. Percentage change in inflows at Rawal Dam under Scenario B (i.e., current climate and future land use).

	Flows (Future Land Use Present Climate) (2016–2100)	
	cusecs	% change
Observed	129.5	-
Simulated	174.6	34.8

Figure 11 relates mean monthly flows over the baseline period (1990–2015) to those for anticipated flows with changing land use to look at the temporal variations in the Rawal watershed. With the exception of February and September, when they exhibit a falling tendency, inflows generally show a rising trend throughout the whole year.

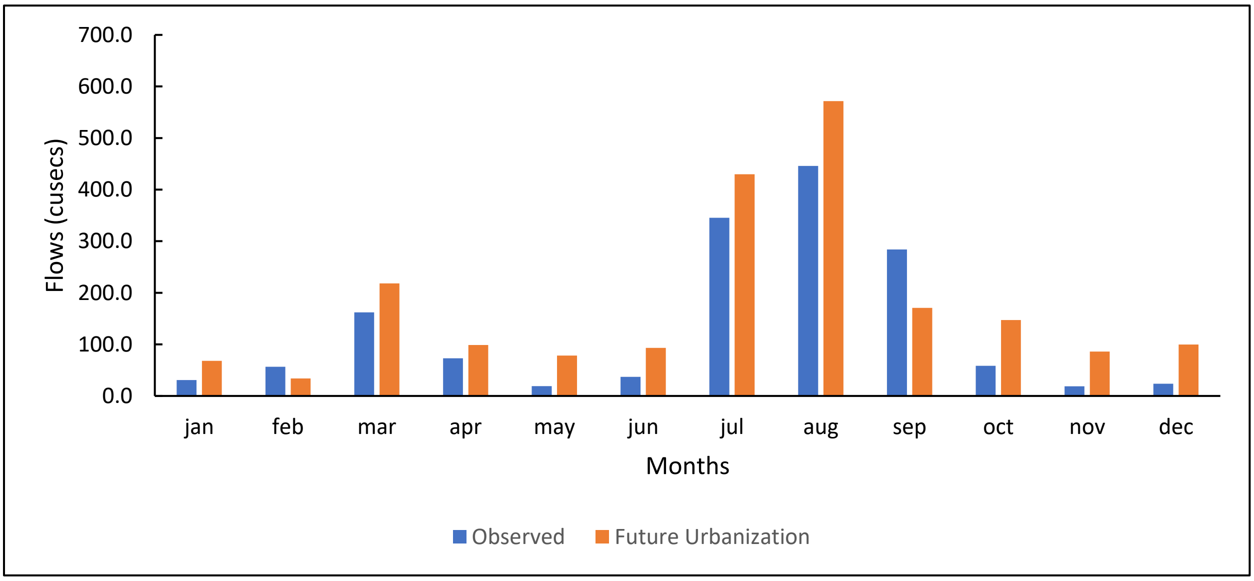

Figure 11. Mean monthly flows at Rawal Dam under current climate and future land use condition.

4.6. Reservoir Operation Simulation

Figure 12 depicts the results of simulating reservoir level using the measured inflow and the initial operating rule curves for 2.05 cumecs. The observed and predicted reservoir levels show a substantial difference. The model's goal is to choose an appropriate water release while keeping the reservoir level within the desired range as specified by operational rule curves. RMSE = 12.6 Mm^3 and R^2 = 0.63 during calibration (2004–2010) and RMSE = 6.11 Mm^3 and R^2 = 0.63 during validation (2011–2013) demonstrate the variability in the yearly aggregate of releases. While comparing these numbers, several factors such as data flow uncertainty and operational control rule breaches need to be taken into consideration.

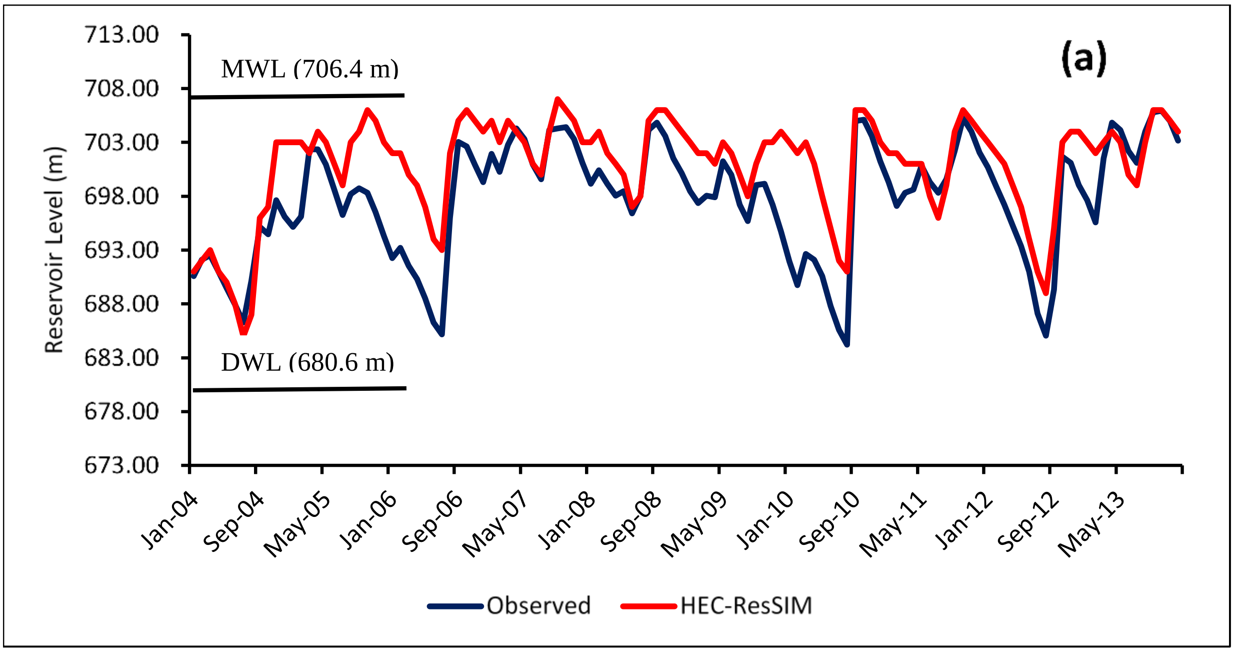

Figure 12. *Cont.*

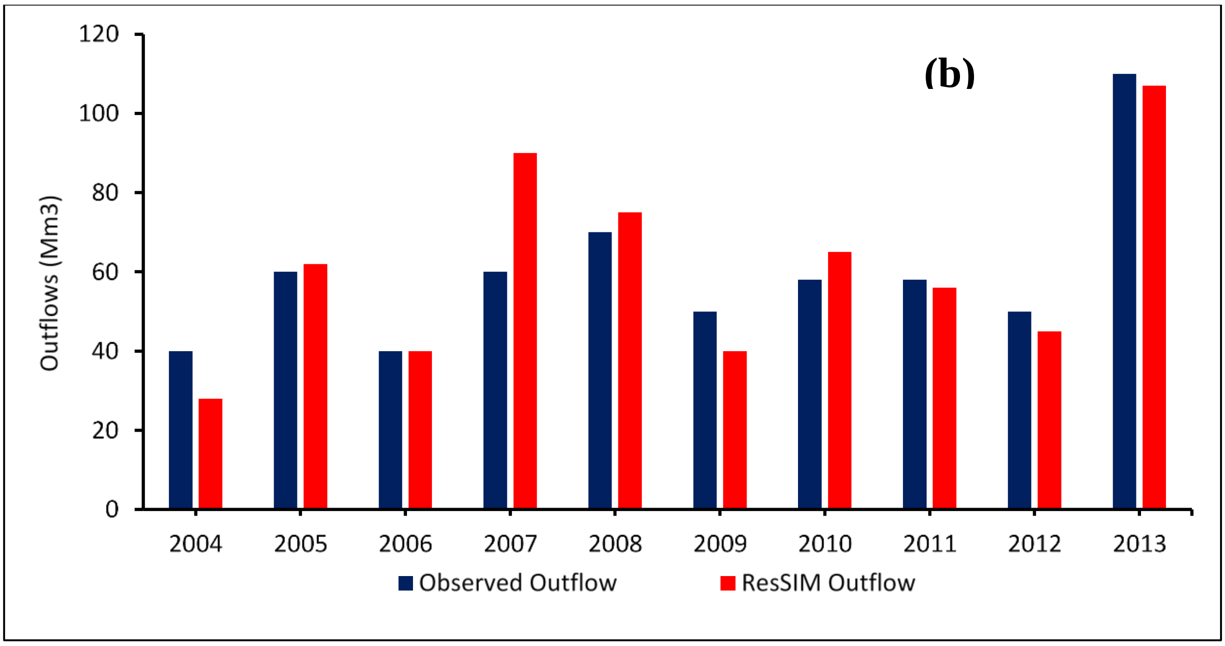

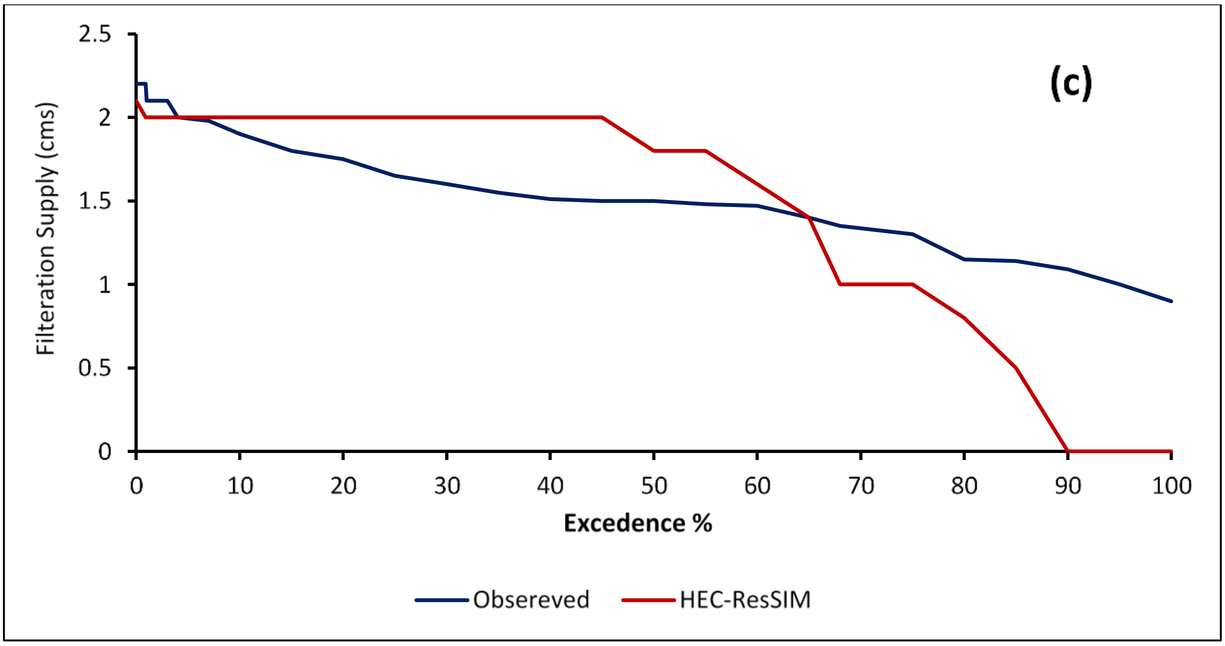

Figure 12. Comparison of measured and simulated data from HEC-ResSIM for the following parameters: (**a**) daily reservoir level, (**b**) annual release (filtration + spillway), and (**c**) flow duration curve of daily filtration supply.

The flow duration curve (Figure 12c) explains the difference between the observed and HEC-ResSIM-modeled filtration discharges for the years 2004 to 2013. It is evident that less than 2.05 cumecs of the water was given less than 10% of the time in prior years. HEC-ResSIM simulations show that supplies of 2.05 cumecs could be obtained for 48% of the time, provided that the operating rule curves are followed, but it is also feasible to encounter zero supply circumstances.

Either the rule curve was not strictly observed in prior years, or the definition of 2.05 cumecs in the rule curve is inaccurate.

Impacts of Climate Change on Reservoir Operational Strategy

Evaluating potential effects of climate change on the operational plan for Rawal reservoir was one of the study's primary goals. The reliability, vulnerability, resilience, and water usage effectiveness of the system were assessed in contrast to four water source plans (SBL, S10, S30, and S50) and the present water level targets. Reliability refers to the ability of a reservoir system to consistently meet the water demands and fulfill its intended purposes over a specified period. It involves ensuring a dependable supply of water for various uses such as agriculture, drinking water, industrial processes, and environmental needs. The reliability of a reservoir operation is typically measured by evaluating the system's capacity to meet water demands under different hydrological conditions and over extended timeframes. In addition, vulnerability in reservoir operation refers to the susceptibility of a system to adverse events or changes that can impact its performance. This can include factors such as climate variability, droughts, extreme precipitation events, or changes in water availability. Reservoirs can be vulnerable to inadequate inflows, which may result in water shortages, reduced power generation, or insufficient water supply for different sectors. Assessing vulnerability helps in identifying potential weaknesses in the system and developing strategies to mitigate risks.

Resilience refers to the ability of a reservoir system to absorb disturbances or shocks and efficiently recover to its desired state. Resilient reservoir operation allows it to adapt to changing conditions, such as sudden shifts in water availability, without compromising its functionality. This can involve strategies like adaptive management, flexible operating rules, and infrastructure improvements to enhance the system's capacity to withstand and bounce back from disruptions.

Water usage effectiveness relates to the efficiency and sustainability of water utilization within a reservoir system. It focuses on optimizing the allocation and distribution of water resources to achieve multiple objectives, such as maximizing water supply, minimizing losses, and considering environmental and social factors. Water usage effectiveness emphasizes responsible water management practices, including efficient irrigation techniques, demand management strategies, and the protection of ecological flows to ensure the equitable and sustainable use of water resources.

Tables 7 and 8 provide an analysis of the system's reliability, resilience, vulnerability, and water usage effectiveness.

With the current operational strategy, there must be a trade-off in performance indicators, and the system's performance does not always hold true, regardless of the circumstances surrounding the water supply. The WUE generally increases over time as baseline water supply increases, but system reliability and resilience steadily decrease. The system's highest dependability is 99.74% when following the baseline water distribution plan (SBL) in the 2055s with SSP5 and the 2025s under SSP2. Nonetheless, the most ambitious water supply plan, S50, achieved the highest WUE under SSP5 and SSP2 for the years 2025 and 2055, respectively, i.e., 67.2% and 65.27%. With an identical water supply plan, SSP2 has the highest system resilience (68.97%) and the lowest vulnerability (20.85) in the 2025s, but SSP5 has the most robust (73.49%) and least susceptible (23.43) circumstances in the 2085s.

Upon consideration, it becomes clear that the operator must be able to discharge the expected volume of water while maintaining a high level of system operation for an extended period of time. The user must maintain the system's high level of dependability and effective use of water resources in order to accomplish this. However, as was already mentioned, system dependability declines as water sources rise. To get a highly dependable system with efficient water consumption, it is recommended to change the existing rule curve.

Table 7. Performance evaluation of the changed rule curve under Shared Socioeconomic Pathway SSP5.

2011–2040 (2025s)								
Emission Scenario	SSP5							
Supply	SBL		S10		S30		S50	
Operational Rule	Present	Modified	Present	Modified	Present	Modified	Present	Modified
Reliability%	99.59	99.64	98.5	99.02	89.22	98.36	79.89	92.11
Resilience%	53.33	53.85	34.76	28.97	19.22	38.89	6.62	16.32
Vulnerability %	63.83	59.55	56.73	54.59	45.14	50.82	49.29	51.58
W.Use Efficiency %	49.63	49.66	54.28	54.44	61.54	64.12	67.2	71.47
2041–2070 (2055s)								
Emission Scenario	SSP5							
Supply	SBL		S10		S30		S50	
Operational Rule	Present	Modified	Present	Modified	Present	Modified	Present	Modified
Reliability%	99.74	99.74	98.46	99.16	90.4	99.09	80.86	97.51
Resilience%	67.86	67.86	41.42	33.7	20.53	48	7.15	19.41
Vulnerability %	59.2	59.2	44.68	36.57	39.22	53.66	47.87	67.06
W.Use Efficiency %	47.97	47.97	52.49	52.51	60.1	61.91	65.42	70.53
2041–2070 (2085s)								
Emission Scenario	SSP5							
Supply	SBL		S10		S30		S50	
Operational Rule	Present	Modified	Present	Modified	Present	Modified	Present	Modified
Reliability%	99.24	99.7	98.54	99.53	92.25	99.47	83.65	99.11
Resilience%	73.49	60.61	64.38	96.15	24.62	55.17	9.99	35.05
Vulnerability %	23.43	59.25	25.21	41.77	34.3	54.62	43.73	25.09
W.Use Efficiency %	41.6	41.6	45.67	45.75	52.71	54	57.99	62.33

Table 8. Performance evaluation of the changed and current rule curves under Shared Socioeconomic Pathway SSP2.

2011–2040 (2025s)								
Emission Scenario	SSP2							
Supply	SBL		S10		S30		S50	
Operational Rule	Present	Modified	Present	Modified	Present	Modified	Present	Modified
Reliability%	99.74	99.74	97.65	99.24	87.92	99.06	80.78	93.01
Resilience%	68.97	68.97	56.2	37.35	15.86	32.04	5.37	11.1
Vulnerability %	52.61	52.61	30.1	43.91	33.91	32.47	43.29	48.61
W.Use Efficiency %	43.97	43.97	48.08	48.28	54.86	57.05	60.46	63.74
2041–2070 (2055s)								
Emission Scenario	SSP2							
Supply	SBL		S10		S30		S50	
Operational Rule	Present	Modified	Present	Modified	Present	Modified	Present	Modified
Reliability%	98.24	99.16	95.03	99.07	86.67	99.14	80.01	97.24
Resilience%	32.12	33.7	31.56	30.39	11.91	47.87	5.98	33.44
Vulnerability %	35.16	38.06	31.28	44.19	35.66	61.67	44.32	56.69
W.Use Efficiency %	47.57	47.73	51.81	52.46	59.18	61.88	65.27	70.6
2041–2070 (2085s)								
Emission Scenario	SSP2							
Supply	SBL		S10		S30		S50	
Operational Rule	Present	Modified	Present	Modified	Present	Modified	Present	Modified
Reliability%	95.36	99.53	91.34	99.44	84.54	99.12	80.92	98.71
Resilience%	28.94	54.9	26.03	60.66	11.92	34.38	7.46	63.83
Vulnerability %	29.75	39.96	31.26	54.6	36.97	42.32	43.99	36.78
W.Use Efficiency %	41.9	42.45	45.43	46.63	51.97	55.06	58.2	63.45

It is essential to remember that effectiveness of the system as a whole increases after applying alterations to the current rule curves. Here, it should be highlighted that operational rule curves play a very essential role and that raising flows alone does not always lead to higher water supply.

The water resources manager will need to select the water delivery plan that best meets the requirements and goals of reservoir operation because it is difficult to achieve ideal circumstances for all performance criteria. However, since Rawal Dam was built specifically for domestic water supplies, a prolonged system breakdown is not acceptable. Therefore, we propose S30 for 2025, 2055, and S50 for 2085, under SSP5, with adaptation of modified operational rule curves shown in Figure 12. This will take care of the aforementioned reservoir operation objectives as well as the expected rise in water demand. Figure 12's modified operational rule curve for SSP2 recommends similar water delivery scenarios for comparable time windows. The there is a significant difference in the 2085s time frame between the modified and present rules, which could be attributed to a shift in the inflow pattern.

5. Discussion

The majority of precipitation comes as snow during the winter, especially in the basin's northern regions. The greatest discharge is recorded in July, according to data on river flow, while average annual inflow measured at the Rawal Dam gauge station is 129.5 cusecs [52,53]. In order to understand how climate change affects river flow regimes, many of the outcomes from the CMIP6 Global Climate Models (GCMs) are considered as a helpful option [52,54–57]. The purpose of this research is to assess how expected shifts in land use and climate will impact flows in the Marghalla Mountains' catchment region of the Rawal Dam. To assess the temporal impacts of expected land use and climate change, the calibrated HEC-HMS hydrological model was created. The chosen GCM's (MPI-ESM1-2-HR) downscaled projections of the baseline period's temperature and precipitation were in excellent agreement with the predictions made using gauge-based observations (1990–2015). This may be due to the CMIP6 models' greatly improved capacity to forecast precipitation and temperature across the Karakoram, Himalaya and Hindukush Regions [37–40,58,59]. Statistical downscaling techniques are used in this study; however, it is important to recognize the limitations and drawbacks associated with statistical downscaling techniques. One major drawback is the assumption of stationarity. Statistical downscaling assumes that the relationship between large-scale climate predictors and local-scale climate variables remains constant over time. However, in a changing climate, this assumption may not hold true, leading to potential inaccuracies in downscaling results. Additionally, statistical downscaling relies on historical observations and relationships, which may not fully capture future climate scenarios. The downscaling process also introduces uncertainties due to errors in the input data, limitations of the statistical models used, and assumptions made during the downscaling process. Furthermore, statistical downscaling may struggle to capture extreme events or rare occurrences accurately. Similarly, even though HEC-HMS is a widely used hydrological modeling software that offers various capabilities for simulating and analyzing rainfall-runoff processes. However, it is essential to be aware of the limitations and potential drawbacks of HEC-HMS when utilizing it in hydrological modeling studies. Firstly, HEC-HMS relies on simplified representations of hydrological processes, which may not fully capture the complexity and variability of real-world conditions. This can lead to limitations in accurately modeling specific phenomena, such as complex channel routing or groundwater interactions. Secondly, HEC-HMS requires a significant amount of input data, including rainfall data, watershed characteristics, and soil properties. The accuracy and availability of these data can impact the reliability of the model outputs, and incomplete or erroneous data may introduce uncertainties.

The GCM output analysis (MPI-ESM1-2-HR) results showed ongoing warming on annual and seasonal timeframes over the catchment area of Rawal Dam in the twenty-first century, which is consistent with the results in nearby South Asian regions of the Tibetan Plateau [59,60] and Himalayas [49,52,61]. The local environment's increased levels of greenhouse gases and aerosols may be a factor in the HKH Mountains' significantly higher temperatures [62,63]. In the future (2016–2100), more precipitation is anticipated annually on average. A rise in the Yellow River basin's headwaters was also noted between the years 2015 and 2100 [53]. The GCM forecasts a general increase in precipitation during the future period, with the highest increases expected in the summer and fall. These findings disagree with those from the upper Cruz River basin and Kelantan River basin in Malaysia [64,65]. A paradox was also discovered by Ozturk et al. [66], which is the pattern where summer precipitation tends to diminish in areas with strong westerlies (Afghanistan and Iran). However, the study area's seasonal precipitation trends resemble those that of Karakoram and Himalayan ranges. According to Babur et al. [49], the annual and seasonal precipitation trends in the Himalayan Range's Jhelum River basin are constantly rising. Garee et al. [57] and Masood et al. [25] anticipated that both inter-annual and seasonal precipitation would indicate a greater propensity to rain over the Karakoram Range, in Hunza River basin. These data parallels may be explained by the predominant circulation pattern of westerlies in the Hindukush Range [62,67–69]. Another element causing these parallels in precipitation behavior is the elevated concentration of anthropogenic absorbing aerosols in South Asian atmosphere [70,71].

An analysis of projected flows from the HEC-HMS model shows that annual average flow across both SSPs (SSP2 and SSP5) is rising over the course of future time frames. Future flow increases could be related to expected growth in annual rainfall and the warming of the climate. According to predictions, the Indus River and Swat River levels will both rise, as reported by Immerzeel et al. [72] and Masood et al. [25], respectively.

6. Conclusions

The Rawal Dam catchment's hydrological response to historical precipitation was simulated using HEC-HMS, and the calibrated model was subsequently used to determine how climate change and land use change would affect reservoir inflows. The Rawal Dam watershed was divided into six sub-basins by the HEC-HMS hydrological model, each with its own unique features. To cover the entire reservoir catchment region, three climate stations were chosen: Murree, Islamabad (zero point) and Rawal Dam. For the time periods of 2003–2005 and 2006–2007, the model was calibrated and confirmed. After calibration, the model's parameters were modified, and the calibrated model was then used for confirmation. The measured and simulated reservoir levels were well matched by the model. Then, utilizing statistical downscaling of data generated by GCM (MPI-ESM1-2-HR), the CMhyd model used climate change precipitation predictions for both Shared Socioeconomic Pathways (SSPs) 2 and 5. Projections were added to the calibrated model after downscaling in order to determine any possible effects of climate change on Rawal Dam. For the baseline (1990–2015) and (2016–2100), which encompassed the current century, the analysis was performed on a seasonal basis. The following are some findings from the research:

- In comparison to the baseline period (1990–2015), the Rawal Dam catchment's annual minimum, maximum, and mean temperatures and precipitation have been rising steadily since 2016. Future streamflows are influenced by the higher precipitation.
- Under current land use and land cover conditions, it is expected that the average daily streamflow at Rawal Dam will rise from 129.5 cusecs (1990–2015) to 151.9 cusecs under SSP2 and to 160.5 cusecs under SSP5.
- While this flow grew from 129.5 cusecs (1990–2015) to 177.1 cusecs under current climate conditions and future land use and land cover scenarios.
- The findings showed that while mean monthly flows have risen overall, those for December and February have decreased.

This research expanded our understanding of the effects of CC and land use land cover change on Rawal Dam catchment and indicated that these effects are important enough that project managers and planners should take these effects into account when developing their long-term operational plans.

While the current study concentrates on effects of CC and land use land cover changes on streamflow, future research on the effects on the basin's groundwater and sediment dynamics may also be taken into consideration. Additionally, a sensitivity analysis and a spatial analysis of dam operation policies under climate change could be considered for future studies.

Author Contributions: All authors were involved in the intellectual elements of this paper. S.H. (Sharjeel Hassan), M.U.M., S.H. (Saif Haider), Y.D., D.S. and M.N.A. designed the research. F.H., S.H. (Saif Haider) and M.U.M. conducted the research and wrote the manuscript. M.R. and M.U.N. helped in the data arrangement and analysis. All authors have read and agreed to the published version of the manuscript.

Funding: This study was supported by the International Partnership Program of Chinese Academy of Sciences (Grant No. 131551KYSB20200022).

Data Availability Statement: The data are not publicly available due to further research.

Conflicts of Interest: The authors declare no conflict of interest.

References

1. Higashi, H.; Dairaku, K.; Matsuura, T. Impacts of Global Warming on Heavy Precipitation Frequency and Flood Risk. *Proc. Hydraul. Eng.* **2006**, *50*, 205–210. [CrossRef]
2. Watkins, K. Human Development Report 2006—Beyond Scarcity: Power, Poverty and the Global Water Crisis. *Soc. Sci. Res. Netw.* **2006**, *44*, 44-6944. [CrossRef]
3. Vörösmarty, C.J.; McIntyre, P.B.; Gessner, M.O.; Dudgeon, D.; Prusevich, A.; Green, P.; Glidden, S.; Bunn, S.E.; Sullivan, C.A.; Liermann, C.R.; et al. Global threats to human water security and river biodiversity. *Nature* **2010**, *467*, 555–561. [CrossRef]
4. Mahmood, S.; Kiliç, Z.; Saeed, M.M.; Rehman, H.A.; Aslan, Z.; Elsarag, E.I.; Ahmad, I.; Haider, S. Environmental and Hydrological Consequences of Agriculture Activities: General Review & Case Study Environmental and Hydrological Consequences of Agriculture Activities. *Int. J. Water Resour. Arid Environ.* **2022**, *11*, 43–61.
5. Haider, S.; Masood, M.U. Analyzing frequency of Floods in Upper Indus Basin under various Climate Change Scenarios. In Proceedings of the 2nd National Conference on Sustainable Water Resources Management (SWRM-22), Lahore, Pakistan, 16 November 2022; pp. 137–141.
6. Kochhar, K.; Pattillo, C.; Sun, Y.; Suphaphiphat, N.; Swiston, A.; Tchaidze, R.; Clements, B.; Fabrizio, S.; Flamini, V.; Redifer, L.; et al. Is the Glass Half Empty Or Half Full?: Issues in Managing Water Challenges and Policy Instruments. *Staff Discuss. Notes* **2015**, *15*, 1. [CrossRef]
7. Gedney, N.; Cox, P.M.; Betts, R.A.; Boucher, O.; Huntingford, C.; Stott, P.A. Detection of a direct carbon dioxide effect in continental river runoff records. *Nature* **2006**, *439*, 835–838. [CrossRef] [PubMed]
8. Lee, K.S.; Chung, E.-S. Hydrological effects of climate change, groundwater withdrawal, and land use in a small Korean watershed. *Hydrol. Process.* **2007**, *21*, 3046–3056. [CrossRef]
9. Shi, X.; Wang, W.; Shi, W. Progress on quantitative assessment of the impacts of climate change and human activities on cropland change. *J. Geogr. Sci.* **2016**, *26*, 339–354. [CrossRef]
10. Iqbal, M.; Wen, J.; Masood, M.; Masood, M.U.; Adnan, M. Impacts of Climate and Land-Use Changes on Hydrological Processes of the Source Region of Yellow River, China. *Sustainability* **2022**, *14*, 14908. [CrossRef]
11. Shabahat, S.; Raza, A.; Haider, S.; Masood, M.U.; Rashid, M. Investigating the Groundwater Recharge Potential in the Upper Rechna Doab. In Proceedings of the 2nd National Conference on Sustainable Water Resources Management (SWRM-22), Lahore, Pakistan, 16 November 2022; pp. 100–107.
12. Jaffry, A.H.; Raza, H.; Haider, S.; Masood, M.U.; Waseem, M.; Shahid, M.A.; Ali, B. Comparison between the Remote Sensing-based drought indices in Punjab, Pakistan. In Proceedings of the 2nd National Conference on Sustainable Water Resources Management (SWRM-22), Lahore, Pakistan, 16 November 2022; pp. 94–99.
13. Nagra, M.; Masood, M.U.; Haider, S.; Rashid, M. Assessment of Spatiotemporal Droughts Through Machine Learning Algorithm Over Pakistan. In Proceedings of the 2nd National Conference on Sustainable Water Resources Management (SWRM-22), Lahore, Pakistan, 16 November 2022; pp. 32–43.
14. Du, J.; Qian, L.; Rui, H.; Zuo, T.; Zheng, D.; Xu, Y.; Xu, C.-Y. Assessing the effects of urbanization on annual runoff and flood events using an integrated hydrological modeling system for Qinhuai River basin, China. *J. Hydrol.* **2012**, *464*, 127–139. [CrossRef]
15. Tomer, M.D.; Schilling, K.E. A simple approach to distinguish land-use and climate-change effects on watershed hydrology. *J. Hydrol.* **2009**, *376*, 24–33. [CrossRef]
16. Zohaib, M.; Kim, H.; Choi, M. Evaluating the patterns of spatiotemporal trends of root zone soil moisture in major climate regions in East Asia. *J. Geophys. Res. Atmos.* **2017**, *122*, 7705–7722. [CrossRef]

17. Liang, W.; Bai, D.; Wang, F.; Fu, B.; Yan, J.; Wang, S.; Yang, Y.; Long, D.; Feng, M. Quantifying the impacts of climate change and ecological restoration on streamflow changes based on a Budyko hydrological model in China's Loess Plateau. *Water Resour. Res.* **2015**, *51*, 6500–6519. [CrossRef]
18. Trail, M.; Tsimpidi, A.; Liu, P.; Tsigaridis, K.; Hu, Y.; Nenes, A.; Stone, B.; Russell, A. Potential Impact of Land Use Change on Future Regional Climate in the Southeastern U.S.: Reforestation and Crop Land Conversion. *J. Geophys. Res. Atmos.* **2013**, *118*, 11577–11588. [CrossRef]
19. Fohrer, N.; Haverkamp, S.; Frede, H.-G. Assessment of the effects of land use patterns on hydrologic landscape functions: Development of sustainable land use concepts for low mountain range areas. *Hydrol. Process.* **2005**, *19*, 659–672. [CrossRef]
20. Nasseri, M.; Zahraie, B.; Ajami, N.; Solomatine, D. Monthly water balance modeling: Probabilistic, possibilistic and hybrid methods for model combination and ensemble simulation. *J. Hydrol.* **2014**, *511*, 675–691. [CrossRef]
21. Li, Z.; Fang, H. Modeling the impact of climate change on watershed discharge and sediment yield in the black soil region, northeastern China. *Geomorphology* **2017**, *293*, 255–271. [CrossRef]
22. Fernandez, W.; Vogel, R.M.; Sankarasubramanian, A. Regional calibration of a watershed model. *Hydrol. Sci. J.* **2000**, *45*, 689–707. [CrossRef]
23. Shahid, M.; Cong, Z.; Zhang, D. Understanding the impacts of climate change and human activities on streamflow: A case study of the Soan River basin, Pakistan. *Theor. Appl. Climatol.* **2017**, *134*, 205–219. [CrossRef]
24. Vonk, E.; Xu, Y.P.; Booij, M.J.; Zhang, X.; Augustijn, D.C.M. Adapting multireservoir operation to shifting patterns of water supply and demand: A case study for the Xinanjiang-Fuchunjiang reservoir cascade. *Water Resour. Manag.* **2014**, *28*, 625–643. [CrossRef]
25. Masood, M.U.; Khan, N.M.; Haider, S.; Anjum, M.N.; Chen, X.; Gulakhmadov, A.; Iqbal, M.; Ali, Z.; Liu, T. Appraisal of Landcover and Climate Change Impact on Water Resources: A Case Study of Mohmand Dam Catchment, Pakistan. *Water* **2023**, *15*, 1313. [CrossRef]
26. Wei, X.; Liu, W.; Zhou, P. Quantifying the relative contributions of forest change and climatic variability to hydrology in large watersheds: A critical review of research methods. *Water* **2013**, *5*, 728–746. [CrossRef]
27. Tahir, A.A.; Chevallier, P.; Arnaud, Y.; Ahmad, B. Snow cover dynamics and hydrological regime of the Hunza River basin, Karakoram Range, Northern Pakistan. *Hydrol. Earth Syst. Sci.* **2011**, *15*, 2275–2290. [CrossRef]
28. Ahmed, N.; Wang, G.; Booij, M.J.; Xiangyang, S.; Hussain, F.; Nabi, G. Separation of the Impact of Landuse/Landcover Change and Climate Change on Runoff in the Upstream Area of the Yangtze River, China. *Water Resour. Manag.* **2022**, *36*, 181–201. [CrossRef]
29. Yang, L.; Feng, Q.; Yin, Z.; Deo, R.C.; Wen, X.; Si, J.; Li, C. Separation of the Climatic and Land Cover Impacts on the Flow Regime Changes in Two Watersheds of Northeastern Tibetan Plateau. *Adv. Meteorol.* **2017**, *2017*, 6310401. [CrossRef]
30. Sinha, R.K.; Eldho, T.I.; Subimal, G. Assessing the impacts of land use/land cover and climate change on surface runoff of a humid tropical river basin in Western Ghats, India. *Int. J. River Basin Manag.* **2020**, *21*, 141–152. [CrossRef]
31. Nickman, A.; Lyon, S.W.; Jansson, P.-E.; Olofsson, B. Simulating the impact of roads on hydrological responses: Examples from Swedish terrain. *Hydrol. Res.* **2016**, *47*, 767–781. [CrossRef]
32. Rahman, K.U.; Balkhair, K.S.; Almazroui, M.; Masood, A. Sub-catchments flow losses computation using Muskingum–Cunge routing method and HEC-HMS GIS based techniques, case study of Wadi Al-Lith, Saudi Arabia. *Model. Earth Syst. Environ.* **2017**, *3*, 4. [CrossRef]
33. Wang, G.; Zhang, J.; Pagano, T.C.; Xu, Y.; Bao, Z.; Liu, Y.; Jin, J.; Liu, C.; Song, X.; Wan, S. Simulating the hydrological responses to climate change of the Xiang River basin, China. *Theor. Appl. Climatol.* **2015**, *124*, 769–779. [CrossRef]
34. Chu, X.; Steinman, A. Event and Continuous Hydrologic Modeling with HEC-HMS. *J. Irrig. Drain. Eng.* **2009**, *135*, 119–124. [CrossRef]
35. Tassew, B.G.; Belete, M.A.; Miegel, K. Application of HEC-HMS Model for Flow Simulation in the Lake Tana Basin: The Case of Gilgel Abay Catchment, Upper Blue Nile Basin, Ethiopia. *Hydrology* **2019**, *6*, 21. [CrossRef]
36. Gunacti, M.C.; Gul, G.O.; Cetinkaya, C.P.; Gul, A.; Barbaros, F. Evaluating Impact of Land Use and Land Cover Change Under Climate Change on the Lake Marmara System. *Water Resour. Manag.* **2022**, *37*, 2643–2656. [CrossRef]
37. Azizi, S.; Ilderomi, A.R.; Noori, H. Investigating the effects of land use change on flood hydrograph using HEC-HMS hydrologic model (case study: Ekbatan Dam). *Nat. Hazards* **2021**, *109*, 145–160. [CrossRef]
38. Azmat, M.; Qamar, M.U.; Huggel, C.; Hussain, E. Future climate and cryosphere impacts on the hydrology of a scarcely gauged catchment on the Jhelum river basin, Northern Pakistan. *Sci. Total Environ.* **2018**, *639*, 961–976. [CrossRef]
39. Candela, L.; Tamoh, K.; Olivares, G.; Gomez, M. Modelling impacts of climate change on water resources in ungauged and data-scarce watersheds. Application to the Siurana catchment (NE Spain). *Sci. Total Environ.* **2012**, *440*, 253–260. [CrossRef] [PubMed]
40. Verma, A.K.; Jha, M.K.; Mahana, R.K. Evaluation of HEC-HMS and WEPP for simulating watershed runoff using remote sensing and geographical information system. *Paddy Water Environ.* **2009**, *8*, 131–144. [CrossRef]
41. Zelelew, D.G.; Melesse, A.M. Applicability of a Spatially Semi-Distributed Hydrological Model for Watershed Scale Runoff Estimation in Northwest Ethiopia. *Water* **2018**, *10*, 923. [CrossRef]
42. Karlsson, I.B.; Sonnenborg, T.O.; Refsgaard, J.C.; Trolle, D.; Børgesen, C.D.; Olesen, J.E.; Jeppesen, E.; Jensen, K.H. Combined effects of climate models, hydrological model structures and land use scenarios on hydrological impacts of climate change. *J. Hydrol.* **2016**, *535*, 301–317. [CrossRef]

43. Li, B.; Li, C.; Liu, J.; Zhang, Q.; Duan, L. Decreased streamflow in the Yellow River basin, China: Climate change or human-induced? *Water* **2017**, *9*, 116. [CrossRef]
44. Liu, L.; Liu, Z.; Ren, X.; Fischer, T.; Xu, Y. Hydrological impacts of climate change in the Yellow River Basin for the 21st century using hydrological model and statistical downscaling model. *Quat. Int.* **2011**, *244*, 211–220. [CrossRef]
45. Ahmadalipour, A.; Rana, A.; Moradkhani, H.; Sharma, A. Multi-Criteria Evaluation of CMIP5 GCMs for Climate Change Impact Analysis. *Theor. Appl. Climatol.* **2015**, *128*, 71–87. [CrossRef]
46. Rozenberg, J.; Davis, S.J.; Narloch, U.; Hallegatte, S. Climate constraints on the carbon intensity of economic growth. *Environ. Res. Lett.* **2015**, *10*, 95006. [CrossRef]
47. Anandhi, A.; Frei, A.; Pierson, D.C.; Schneiderman, E.M.; Zion, M.S.; Lounsbury, D.; Matonse, A.H. Examination of change factor methodologies for climate change impact assessment. *Water Resour. Res.* **2011**, *47*. [CrossRef]
48. Moriasi, D.N.; Arnold, J.G.; van Liew, M.W.; Bingner, R.L.; Harmel, R.D.; Veith, T.L. Model Evaluation Guidelines for Systematic Quantification of Accuracy in Watershed Simulations. *Trans. ASABE* **2007**, *50*, 885–900. [CrossRef]
49. Babur, M.; Babel, M.S.; Shrestha, S.; Kawasaki, A.; Tripathi, N.K. Assessment of Climate Change Impact on Reservoir Inflows Using Multi Climate-Models under RCPs—The Case of Mangla Dam in Pakistan. *Water* **2016**, *8*, 389. [CrossRef]
50. Klipsch, J.D.; Hurst, M.B. HEC-ResSim User's Manual. 2013, p. 556. Available online: https://www.hec.usace.army.mil/software/hec-ressim/documentation/HEC-ResSim_31_UsersManual.pdf (accessed on 7 May 2023).
51. Park, J.Y.; Kim, S.J. Potential impacts of climate change on the reliability of water and hydropower supply from a multipurpose dam in south korea. *J. Am. Water Resour. Assoc.* **2014**, *50*, 1273–1288. [CrossRef]
52. Nasim, W.; Amin, A.; Fahad, S.; Awais, M.; Khan, N.; Mubeen, M.; Wahid, A.; Rehman, M.H.; Ihsan, M.Z.; Ahmad, S.; et al. Future risk assessment by estimating historical heat wave trends with projected heat accumulation using SimCLIM climate model in Pakistan. *Atmos. Res.* **2018**, *205*, 118–133. [CrossRef]
53. Zhang, Y.; Su, F.; Hao, Z.; Xu, C.; Yu, Z.; Wang, L.; Tong, K. Impact of projected climate change on the hydrology in the headwaters of the Yellow River basin. *Hydrol. Process.* **2015**, *29*, 4379–4397. [CrossRef]
54. Anjum, M.N.; Ding, Y.; Shangguan, D.; Ijaz, M.W.; Zhang, S. Evaluation of High-Resolution Satellite-Based Real-Time and Post-Real-Time Precipitation Estimates during 2010 Extreme Flood Event in Swat River Basin, Hindukush Region. *Adv. Meteorol.* **2016**, *2016*, 2604980. [CrossRef]
55. Chen, L.; Frauenfeld, O.W. Surface Air Temperature Changes over the Twentieth and Twenty-First Centuries in China Simulated by 20 CMIP5 Models. *J. Clim.* **2014**, *27*, 3920–3937. [CrossRef]
56. Mahmood, R.; Jia, S. Assessment of Impacts of Climate Change on the Water Resources of the Transboundary Jhelum River Basin of Pakistan and India. *Water* **2016**, *8*, 246. [CrossRef]
57. Garee, K.; Chen, X.; Bao, A.; Wang, Y.; Meng, F. Hydrological modeling of the upper indus basin: A case study from a high-altitude glacierized catchment Hunza. *Water* **2017**, *9*, 17. [CrossRef]
58. Kent, C.; Chadwick, R.; Rowell, D.P. Understanding uncertainties in future projections of seasonal tropical precipitation. *J. Clim.* **2015**, *28*, 4390–4413. [CrossRef]
59. Yang, T.; Hao, X.; Shao, Q.; Xu, C.-Y.; Zhao, C.; Chen, X.; Wang, W. Multi-model ensemble projections in temperature and precipitation extremes of the Tibetan Plateau in the 21st century. *Glob. Planet. Chang.* **2012**, *80*, 1–13. [CrossRef]
60. You, Q.; Min, J.; Kang, S. Rapid warming in the Tibetan Plateau from observations and CMIP5 models in recent decades. *Int. J. Climatol.* **2015**, *36*, 2660–2670. [CrossRef]
61. Dimri, A.; Kumar, D.; Choudhary, A.; Maharana, P. Future changes over the Himalayas: Maximum and minimum temperature. *Glob. Planet. Chang.* **2018**, *162*, 212–234. [CrossRef]
62. Anjum, M.N.; Ding, Y.; Shangguan, D.; Ahmad, I.; Ijaz, M.W.; Farid, H.U.; Yagoub, Y.E.; Zaman, M.; Adnan, M. Performance evaluation of latest integrated multi-satellite retrievals for Global Precipitation Measurement (IMERG) over the northern highlands of Pakistan. *Atmos. Res.* **2018**, *205*, 134–146. [CrossRef]
63. Bollasina, M.A.; Ming, Y.; Ramaswamy, V. Anthropogenic Aerosols and the Weakening of the South Asian Summer Monsoon. *Science* **2011**, *334*, 502–505. [CrossRef]
64. Shamir, S.B.; Carrillo, C.M.; Castro, C.L.; Chang, H.I.; Chief, K.; Corkhill, F.E.; Eden, S.; Georgakakos, K.P.; Nelson, K.M.; Prietto, J. Climate change and water resources management in the Upper Santa Cruz River, Arizona. *J. Hydrol.* **2015**, *521*, 18–33. [CrossRef]
65. Tan, M.L.; Yusop, Z.; Chua, V.P.; Chan, N.W. Climate change impacts under CMIP5 RCP scenarios on water resources of the Kelantan River Basin, Malaysia. *Atmos. Res.* **2017**, *189*, 1–10. [CrossRef]
66. Ozturk, T.; Turp, M.T.; Türkeş, M.; Kurnaz, M.L. Projected changes in temperature and precipitation climatology of Central Asia CORDEX Region 8 by using RegCM4.3.5. *Atmos. Res.* **2017**, *183*, 296–307. [CrossRef]
67. Gan, R.; Zuo, Q. Assessing the digital filter method for base flow estimation in glacier melt dominated basins. *Hydrol. Process.* **2015**, *30*, 1367–1375. [CrossRef]
68. Anjum, M.N.; Ding, Y.; Shangguan, D.; Liu, J.; Ahmad, I.; Ijaz, M.W.; Khan, M.I. Quantification of spatial temporal variability of snow cover and hydro-climatic variables based on multi-source remote sensing data in the Swat watershed, Hindukush Mountains, Pakistan. *Meteorol. Atmos. Phys.* **2018**, *131*, 467–486. [CrossRef]
69. Dahri, Z.H.; Ludwig, F.; Moors, E.; Ahmad, B.; Khan, A.; Kabat, P. An appraisal of precipitation distribution in the high-altitude catchments of the Indus basin. *Sci. Total Environ.* **2016**, *548*, 289–306. [CrossRef]

70. Kaskaoutis, D.; Houssos, E.; Solmon, F.; Legrand, M.; Rashki, A.; Dumka, U.; Francois, P.; Gautam, R.; Singh, R. Impact of atmospheric circulation types on southwest Asian dust and Indian summer monsoon rainfall. *Atmos. Res.* **2018**, *201*, 189–205. [CrossRef]
71. Xin, J.; Gong, C.; Wang, S.; Wang, Y. Aerosol direct radiative forcing in desert and semi-desert regions of northwestern China. *Atmos. Res.* **2016**, *171*, 56–65. [CrossRef]
72. Lutz, A.F.; Immerzeel, W.W.; Shrestha, A.B.; Bierkens, M.F.P. Consistent increase in High Asia's runoff due to increasing glacier melt and precipitation. *Nat. Clim. Chang.* **2014**, *4*, 587–592. [CrossRef]